Annu. Rev. Astron. Astrophys. 1993. 31: 217–63

THE ATMOSPHERES OF URANUS AND NEPTUNE

Jonathan I. Lunine

Lunar and Planetary Laboratory, University of Arizona, Tucson, Arizona 85721

KEY WORDS: composition, outer planets

INTRODUCTION

Uranus and Neptune are the two outermost giant planets, often classified with Jupiter and Saturn by virtue of being distinct from the inner terrestrial planets. Yet Uranus and Neptune form a class by themselves, composed largely of the rock and ice forming (Z) elements—with hydrogen and helium comprising no more than 15–20% of the mass (Podolak et al 1990, Hubbard et al 1991). This is in contrast to Jupiter and Saturn, which are largely hydrogen and helium, and implies differences in formation conditions, interior dynamics, and atmospheric composition between the "inner" and "outer" pair of giants. Uranus and Neptune are similar in mass (4.3×10^{-5} and 5.1×10^{-5} solar masses, respectively) and density (1.29 and 1.64 g cm^{-3}, respectively) (Zharkov & Gudkova 1991). Their bulk compositions and internal structures are also rather similar (Hubbard et al 1991, Podolak et al 1990), which has important implications for the rather different heat flows out of the atmospheres as explored below.

The atmospheres of Uranus and Neptune are defined here as those levels of the hydrogen-helium envelopes which are generally accessible to observations by remote sensors. Microwave measurements of Uranus and Neptune (Hofstadter & Muhleman 1988, dePater et al 1991) extend down roughly to the 50–100 bar pressure level, and provide a convenient "bottom" to an atmosphere which, in reality, grades continuously into the fluid interior.

This review comes some seven and four years, respectively, after the *Voyager 2* flybys of Uranus and Neptune, at a time when it seems unlikely

0066–4146/93/0915–0217$02.00

that there will be opportunities for detailed close-in studies of these planets anytime soon. Nonetheless, analysis of *Voyager* data and pursuit of Earth-based studies continues with vigor, and the prospects for using advanced ground-based and Earth-orbital detectors to learn more seem reasonably bright.

The purpose of this chapter is to identify and discuss some of the more interesting aspects of these distant planetary atmospheres which make them worthy of further study. The review is aimed not so much at those who now study these planets as at the larger community of astronomers who may be less familiar with the surprising leaps in knowledge enabled by the *Voyager 2* flybys. Therefore, an exhaustive review of the literature is not attempted; readers desiring such may consult Bergstralh et al (1991) for Uranus (no such review yet exists for Neptune). Historical reviews of the progress of understanding prior to *Voyager 2* can be found in Miner (1991) and Bergstralh (1984). The focus here is on identifying issues of continuing interest and controversy, and less on a complete review. It is to be hoped that the present chapter will encourage more individuals to think about these objects, and perhaps even bring novel observing techniques to bear on the theoretical questions outlined herein.

BASIC OVERVIEW OF THE ATMOSPHERES

To first order, the atmospheres of Uranus and Neptune are similar in terms of temperature structure, composition, and overall dynamics, but possess rather different boundary conditions. The obliquity of Uranus is 98°, while that of Neptune is roughly 29°. Since the radiative cooling timescale in the deeper portion of the atmosphere (roughly at and below 0.1 bar) exceeds the orbital timescale by a large factor, the annual mean component of the insolation dominates (Allison et al 1991). On Uranus more net insolation is received at the poles than the equator, while on Neptune most of the insolation is received at low latitudes. This difference dramatically affects the deep circulation patterns and the distribution of condensable constituents on the two planets. Also, the amount of sunlight at the distance of Neptune is only 2/5 that at Uranus. In spite of this, the effective temperature of the two planets is virtually identical at 59 K, because Neptune has a substantial internal heat flow not associated with insolation, whereas Uranus has little or none (Pearl & Conrath 1991). Many of the detailed differences between the two atmospheres may be caused by the contrasting intensities and patterns of insolation, or in the flux of internal heat (which itself may be altered by how the sunlight is deposited).

Thermal Structure

Figure 1 compares temperature profiles for Uranus and Neptune, based on Lindal et al (1987,1990), Herbert et al (1987), and Bishop et al (1992). A variety of techniques and modeling assumptions have gone into these profiles, which will be discussed in following subsections. The figures are shown at this point to introduce the basic structure of the atmosphere and associated nomenclature. The lower portion of the atmosphere, where the temperature increases with increasing pressure ("negative" temperature gradient), is referred to as the troposphere. The temperature profile in this region is a response to the flow of heat outward from the planet, due both to deep internal heat sources and visible sunlight absorbed and converted to thermal radiation in and below the troposphere itself. Energy transport mechanisms are radiation in the upper troposphere, grading to convection deeper down.

The temperature minimum, at 0.1 bars in the lower two panels of Figure 1, defines the tropopause—the base of the stratosphere, where the temperature increases with altitude, and the energy balance is primarily determined by absorption and emission of radiation. Above the stratosphere lies the thermosphere, in which the thermal structure is governed to first order by molecular conduction, and, at least for the giant planets, the sources of heating are not as yet fully understood. The dividing line between the thermosphere and stratosphere is referred to as the mesopause, and is roughly at a pressure level of 10^{-5}–10^{-4} μbars. It is defined as that level where the column-integrated thermospheric heating rate is balanced exactly by the integrated infrared cooling rate above the mesopause; here the vertical temperature gradient is zero (Strobel et al 1991). Atmospheric levels for Uranus and Neptune are measured also in distance from the 1-bar pressure level obtained through the equation of hydrostatic equilibrium, the temperature profiles in Figure 1, and the basic data in Table 1. An updated temperature profile for the upper atmosphere of Uranus has been constructed very recently by Stevens et al (1993).

By contrast, the Earth's atmospheric structure (from which the nomenclature is derived) exhibits an additional reversal to a negative temperature gradient above the stratosphere and below the thermosphere. This region is called the mesosphere (Figure 2). In Uranus and Neptune the distribution of heating and cooling sources is such that a mesosphere does not occur, and the stratopause and mesopause of Figure 2 may be considered to refer to the same level.

Additional nomenclature used in atmospheric studies refers to the two levels of significance for the kinetic transport of species. The homopause is defined as the level of the atmosphere at which the coefficients of

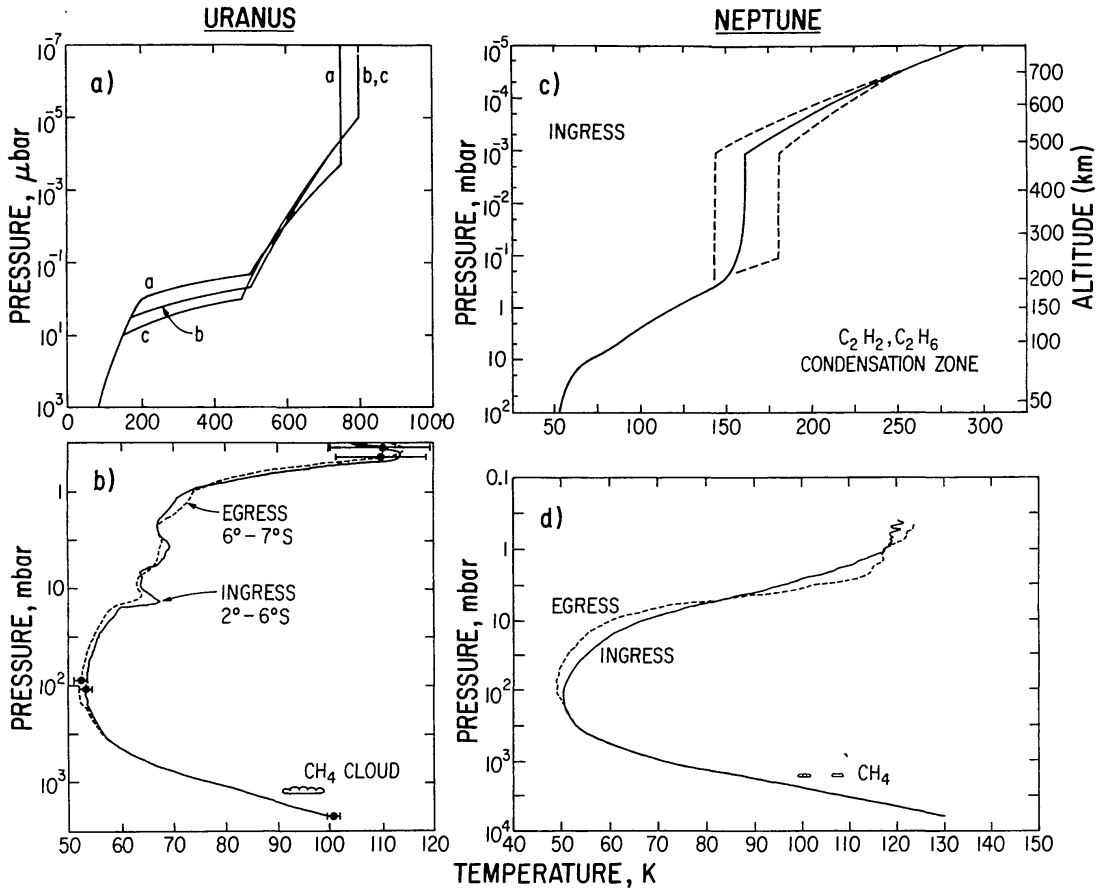

Figure 1 Temperature vs total pressure in the atmospheres of Uranus and Neptune. Left panels apply to Uranus, right to Neptune. (*a*) Temperature profiles in the upper stratosphere and thermosphere of Uranus, as derived from the *Voyager* ultraviolet spectrometer (UVS), from Herbert et al (1987). The three curves correspond to fits to different data sets, and may be considered representative of the uncertainty. Discontinuous breaks in slope are for computational convenience only. At this high level in the atmosphere, molecular hydrogen remains the dominant constituent but not overwhelmingly so; atomic hydrogen becomes competitive at the lowest pressures shown. A very recent update to this portion of the temperature profile may be found in Stevens et al (1993). (*b*) Profile in the stratosphere and troposphere of Uranus, from Lindal et al (1987). The two temperature profiles correspond to two Earth occultation events observed by the radio science subsystem (RSS). The analysis was performed as described in the text; error bars illustrate the uncertainty. (*c*) Stratosphere of Neptune as derived from UVS solar and RSS Earth occultations, from Bishop et al (1992). Dotted lines give a sense of the temperature uncertainty in the stratosphere; discrete break in slope is again a model artifact. (*d*) Stratosphere-troposphere temperature profiles for Neptune, derived from RSS Earth occultations, from Lindal et al (1990). In both lower panels, noise dominates at the top of each profile; high frequency jitter and slope of curve in that region should be disregarded. Note that the temperature profile at and above the mesopause is not shown for Neptune; analysis of *Voyager* data to derive this part of the profile is not yet complete.

Table 1 Basic data on Uranus and Neptune[1]

	Uranus	Neptune
Mean distance from sun (AU)	19.2[(a)]	30.1[(a)]
Obliquity	97°.9[(a)]	28°.8[(a)]
Equatorial radius at 1 bar pressure	25,559 ± 4 km[(b)]	24,764 ± 15 km[(c)]
Rotation rate of magnetic field	17^h24^m[(d)]	16^h11^m[(e)]; 15^h58^m[(f)]
Mass	8.687×10^{28} g[(g)]	1.0243×10^{29} g[(h)]

[1] Data from (*a*) Beatty et al (1981); (*b*) Lindal et al (1987); (*c*) Lindal et al (1990); (*d*) Magnetic field period from Warwick et al (1986); (*e*) Magnetic field period from Warwick et al (1989); (*f*) Correlated motion of Great Dark Spot and south polar features, from Sromovsky & Limaye (1992); (*g*) Tyler et al (1986); (*h*) Tyler et al (1989).

molecular diffusion D and eddy (turbulent) diffusion K are equal; below this level strong vertical mixing dominates while above it molecular species separate diffusively. The eddy coefficient is defined through the one-dimensional equation for the flux F_i of a gas species with number density n_i as (Atreya et al 1991)

$$F_i = \left[-D_i\left(\frac{1}{n_i}\frac{dn_i}{dz} + \frac{1}{H_i} + \frac{(1+\alpha)}{T}\frac{dT}{dz}\right) - K\left(\frac{1}{n_i}\frac{dn_i}{dz} + \frac{1}{H} + \frac{1}{T}\frac{dT}{dz}\right)\right]. \qquad 1.$$

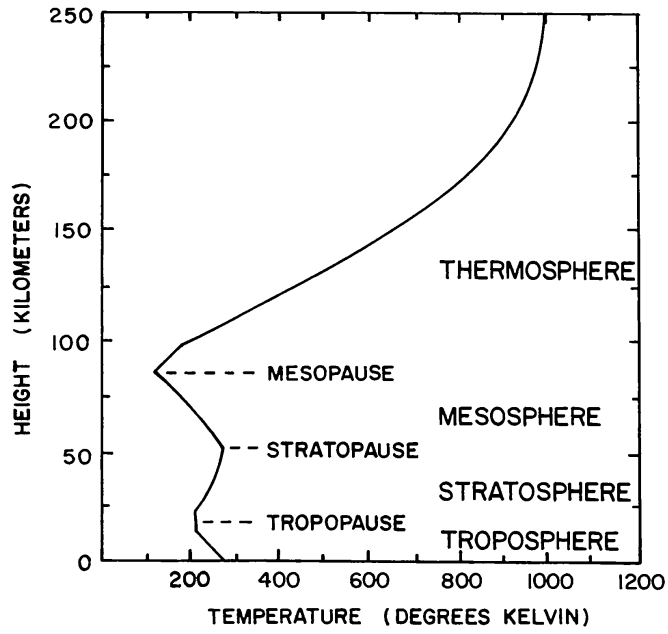

Figure 2 Schematic temperature profile of the Earth's atmosphere, giving the nomenclature for the various portions of the atmosphere based on thermal structure. For Uranus and Neptune, the same terms apply, except that the region between the stratopause and mesopause does not exist. Figure from Chamberlain & Hunten (1987).

Here D_i is the molecular diffusion coefficient for species i, T is the temperature, z the altitude, and α a thermal diffusion factor. $H = RT/mg$ is the pressure scale height, where R is the universal gas constant, g the gravitational acceleration, and m the molecular weight. H refers to the scale height of the particular species when labeled with the subscript i (hence m is m_i); without a subscript it refers to the mean scale height (i.e. the mean molecular weight m is used).

Above the homopause, with $D \gg K$, the first term dominates. Because of its definition in terms of the eddy diffusion coefficient (a measure of the vigor of vertical mixing) the homopause altitude is model dependent, but is located close to the mesopause (Strobel et al 1991). Also, strictly speaking the homopause must be defined for each species, but on Uranus and Neptune it is generally understood to refer to the level at which methane begins to separate diffusively from the background gas. The exobase is the atmospheric level above which the integrated column density produces just one mean free collision path for an atom (Chamberlain & Hunten 1987). Above this level the term exosphere is used to define that tenuous region in which the gas is essentially collisionless.

Composition

To understand the origin of the temperature structures outlined above requires characterizing the sources of opacity, and hence composition. Focusing on the bulk of the atmosphere, the region below the homopause, the primary atmospheric constituent is molecular hydrogen, identified first through the hydrogen dipole lines on Uranus (Herzberg 1952) and since then routinely viewed from the near- through far-infrared (Fegley et al 1991). Molecular hydrogen occurs in both the symmetric (ortho) and antisymmetric (para) spin forms, which have very important consequences for the thermal structure of the troposphere, as discussed below.

Helium represents the most abundant secondary component; its ratio to hydrogen is extremely important from the cosmogonic viewpoint, as described below. Derivation of the helium abundance requires combining data from the radio science subsystem and *Voyager* IRIS (infrared radiometer/interferometric spectrometer) experiment. An occultation of the Earth by Uranus or Neptune seen from *Voyager* provides the opportunity for the radio science subsystem to transmit a pure tone through progressively deeper regions of the atmosphere, and the refraction of the beam is measured on Earth by an apparent change of the position of *Voyager*, yielding a profile of the ratio of atmospheric temperature to molecular weight of the gas. Assuming a constant molecular weight with altitude (except where rapid refractivity variations suggest condensation of a constituent, as discussed below for methane) a family of temperature profiles

corresponding to different molecular weights is generated. These curves are used to generate synthetic infrared spectra, which are compared with actual IRIS spectra to achieve a best fit. The helium abundance is constrained because, once a particular temperature (Figures 1*b* and 1*d*) that best fits the IRIS spectra is selected, the mean molecular weight of the troposphere is determined. Other observations from *Voyager* and ground-based facilities constrain the abundances of elements heavier than helium (with an uncertainty reflected in the error bars reported for the helium abundance). Hence the mean molecular weight derived from the spectral fitting yields the helium abundance (Conrath et al 1991b).

Secondarily, the shape of the IRIS spectra is affected by opacity arising from collisions between hydrogen molecules and helium, which provides an additional (though weaker) constraint on the helium abundance. From this procedure, mass fractions Y of 0.26 ± 0.05 and 0.31 ± 0.05 are determined for Uranus and Neptune, respectively (Conrath et al 1987, 1991b). Marten et al (1993) have argued that N_2 could be the predominant form of nitrogen in Neptune's atmosphere, as discussed below; if it is sufficiently abundant (roughly 0.003 mole fraction) the helium-to-hydrogen ratio on Neptune could be similar to the Uranus value (Conrath et al 1993).

Beyond helium, the search for other constituents is guided by expectations based on elemental abundances measured in the Sun or primitive meteorites (Anders & Grevèsse 1989; Grevesse et al 1991 for carbon abundance), and predictions regarding the partitioning of these species in molecules in the observable atmosphere. Neon is the second most abundant noble gas, but it and the other noble gases are essentially inaccessible by remote observations and await discovery by in situ measurements on entry probes. The three most abundant molecule-forming elements are oxygen, carbon, and nitrogen, in that order. In the hydrogen-rich environment of a giant planet, oxygen forms predominantly water, carbon primarily methane, and nitrogen mostly ammonia; the abundances of these are expressed relative to the solar abundance of the particular Z-element that combines with hydrogen to form them. Thus a "solar abundance of methane" means an amount of methane corresponding to the solar C/H value.

Water condenses out at depths below 15 bars, which are accessible only by ground-based microwave observations. For Uranus, analysis of the data leads inferentially to the presence of a water cloud of sufficient thickness that at least a solar abundance of water is implied below about 50 bars (Hofstadter & Muhleman 1988). The observations are not, however, terribly sensitive to the abundance of water, and on Neptune a deep water abundance is simply assumed in the analysis of the microwave data (de Pater et al 1991).

The microwave observations are much more sensitive to the ammonia abundance, which is a complicated issue tied to the sulfur abundance. Observations from a variety of sources, summarized by de Pater et al (1991), suggest that ammonia is significantly depleted on Uranus relative to solar in a region of the atmosphere (20–40 bars) in which ammonium hydrosulfide particles, NH_4SH, could form. For sulfur to deplete ammonia requires a strong enhancement of the S/N ratio relative to the solar value of 0.16 (Anders & Grevesse 1989). However, wavelengths that probe deeper suggest equatorial enhancement of ammonia and/or other constituents (water and sulfur-bearing species) in the 20-bar or deeper region, grading towards a strong depletion at the pole (de Pater et al 1991). At shorter wavelengths, which probe the 5 to 20 bar region, there also appears to be a decrease in ammonia from mid-latitudes to the pole.

On Neptune, the enhancement of sulfur over its solar value may be as high as 100, but the deep ammonia abundance is not well constrained (de Pater et al 1991). The *Voyager* radio occultation data probed much deeper on Neptune than on Uranus (Lindal et al 1990, Lindal 1992), down to 6 bars, where the ammonia abundance is higher than one would expect above the tops of an ammonia hydrosulfide cloud (de Pater et al 1991). Clearly the situation regarding nitrogen- and sulfur-bearing compounds is a complex one on these two bodies, and an outstanding issue which requires much further work.

Fortunately, the abundance of methane is much better constrained than the other heavy gases, because it is sufficiently volatile that condensation occurs in the high, well-observed portion of the troposphere. Radio occultation results for both Uranus and Neptune (Lindal et al 1987, 1990; Lindal 1992) show evidence of a change in slope of the temperature profile. The base of this change is at 1.2 and 1.9 bars for Uranus and Neptune, respectively, corresponding to a roughly 2% mixing ratio for the derived temperature profile (and using the saturation vapor pressure of methane). Ground-based and *IUE* reflectance observations by Baines & Smith (1990) yield a CH_4 mixing ratio of roughly 3% in the 1-bar region of Neptune's atmosphere; very recent laboratory remeasurement of hydrogen quadrupole lines brings this number down somewhat to 2% (K.H. Baines, personal communication). This mixing ratio represents an enhancement in methane of 10–30 times the solar value. For both planets this abundance is consistent with that determined from ground-based spectroscopic studies of Lutz et al (1976).

Of equal interest is the abundance of methane above its cloud base, since this appears to differ greatly for the two planets. On Uranus the methane abundance up through the tropopause appears to be limited by its saturation vapor pressure, being in fact slightly "undersaturated," in

the sense that its mixing ratio near the tropopause is only 1/2 of the maximum allowed by saturation (Lindal et al 1987). On Neptune, by contrast, methane at the tropopause is the saturated value (roughly 4×10^{-5} mixing ratio) or higher, perhaps by a factor of 10, based on reduction of *Voyager* ultraviolet spectrometer (UVS) data by Bishop et al (1992). An even more recent analysis of the same UVS data by Yelle et al (1993) yields a higher value for methane, $6\text{–}50 \times 10^{-4}$, in the lower stratosphere. This represents methane abundances of order 10–100 times the value corresponding to saturation at the cold trap. Orton et al (1992) made ground-based observations of the 7.8 mm methane emission feature, and found a methane mixing ratio in the stratosphere of $2\text{–}20 \times 10^{-4}$, for stratospheric temperatures between 180 K and 160 K. Baines & Hammel (1992) derived a "nominal" methane mixing ratio in the stratosphere of 3.5×10^{-4} from ground-based reflectance data of Hammel et al (1989).

Earlier ground-based infrared spectroscopy and radiometry, determining both the methane abundance and the tropopause temperature, suggested an even higher oversaturation, by a factor of 100–1000 (Orton & Appleby 1984, Orton et al 1987). Such high values might be ruled out by ground-based optical observations of a stellar occultation by Neptune (Hubbard et al 1987), though these observations are sensitive only to pressures below 1 millibar which is well above the tropopause cold trap. In summary it appears that methane in Neptune's atmosphere is at least saturated at the cold trap, with the bulk of the data suggesting oversaturation by a factor of 10 or so.

The abundances of deuterium-bearing species in the atmospheres of Uranus and Neptune provides important constraints on the relationship of the Z-element component of these bodies to remnant solar system material such as comets and to processes which enhance deuterium in Z-element material in molecular clouds. On Uranus, Trafton & Ramsay (1980) claimed detection of the 4-0 HD line leading to a D/H ratio of $(4.8 \pm 1.5) \times 10^{-5}$, though others have disputed the validity of the detection (see Fegley et al 1991 for a discussion). The detection of several different bands of CH_3D (see, e.g. de Bergh et al 1986) leads to a best value of D/H of 9 $(+9.0, -4.5) \times 10^{-5}$, an uncertainty which reflects both the observational errors and the need to fold in a chemical fractionation factor in going from CH_3D/CH_4 to D/H (Fegley et al 1991). On Neptune, de Bergh et al (1990) found D/H of 1.2 $(+1.2, -0.8) \times 10^{-4}$ from CH_3D. A more recent determination for Neptune, again from CH_3D, yields $D/H = 1.13 \pm 0.16 \times 10^{-4}$ (Orton et al 1992). These values are well in excess of the value in Jupiter and Saturn of around 2×10^{-5} which likely reflects the value in the primordial hydrogen component that forms the bulk of Jupiter and Saturn. The values in Uranus and Neptune then

reflect the enhancement due to incorporation of deuterium-rich ices during formation (Hubbard & MacFarlane 1980, Owen et al 1986, Gautier & Owen 1989, Lutz et al 1990). This is a constraint on the origin of these bodies which we discuss later in the article.

In the stratosphere a number of minor species are to be found, most a result of photochemistry of methane due to influx of ultraviolet photons with wavelengths below 1500 Å, and mostly in solar and interstellar medium Lyman-α (Atreya et al 1991, Broadfoot et al 1989). The dominant hydrocarbon products are expected to be acetylene (or ethyne, C_2H_2) and ethane (C_2H_6). Although ground-based observations provided some information on acetylene abundance and the presence of hazes, conflicting results were obtained (see Atreya et al 1991 for a review). The *Voyager* ultraviolet spectrometer observation of an occultation of the Sun by the atmosphere of Uranus provided information on the acetylene abundance (Broadfoot et al 1986).

The acetylene mixing ratio in the millibar pressure region is roughly 10^{-8}. One-dimensional photochemical models (which relate the gradient of the flux of a photochemical species to the net photochemical production or loss rate) can reproduce the acetylene abundance but cannot simultaneously satisfy data on all the hydrocarbons, indicating the importance of meridional transport which cannot be effectively simulated in such a model (Summers & Strobel 1989). No direct detection of ethane has been made; its presence has been invoked to explain absorption in part of the UVS occultation data (Herbert et al 1987). Overall the abundance of hydrocarbons in the stratosphere of Uranus (including methane) is lower than that on any of the other three giant planets.

On Neptune both ethane and acetylene were detected as emission features in IRIS spectra of the planet (Bézard et al 1991), and ethane has been seen in ground-based data. An additional photochemical product of methane, C_2H_4 (ethene or ethylene), has been tentatively identified from *Voyager* IRIS data (Maguire 1992). The ethane mixing ratio, if it were constant with height, is roughly 10^{-6} from *Voyager* IRIS and ground-based data (Kostiuk et al 1992). Acetylene is lower by a factor of 5–10 (Bézard et al 1991). Retrieval uncertainties and the low effective vertical resolution of the observations (i.e. broad infrared weighting function) prevent direct retrieval of the altitude profile; however ethane and acetylene profiles from photochemical models can be compared with the data for consistency.

An input to the photochemical models which must be adjusted to fit the observed hydrocarbon abundances is the eddy diffusion coefficient K introduced above, because through Equation 1 it determines the rate at which species are advected into and out of photochemically active regions—which are generally below the homopause. The best fits of the

photochemical models to the data yield a value of K of 10^4 cm^2s^{-1} at the Uranus homopause (20 μbar for that value of K), decreasing with altitude proportional to the inverse square root of the atmospheric number density—a standard assumption (Atreya et al 1991). Summers & Strobel (1989) concluded that at the equator, $K \sim 3 \times 10^3$ cm^2s^{-1}; whereas at the sunlit pole K is ~ 50 cm^2s^{-1}. McMillan & Strobel (1992) showed that meridional circulation, in conjunction with the weak vertical mixing implied by the values of K, could account for the observed meridional and vertical distribution of hydrocarbons.

On Neptune, a comprehensive analysis of the *Voyager* ultraviolet solar occultation data places constraints on both the methane abundance and K. Bishop et al (1992) conclude from this analysis that the value of K at the homopause lies between 5×10^6 and 5×10^7 cm^2s^{-1}, the large range being due to uncertainty in the assumed model atmospheric temperature profile. For the nominal case, K of 1–2 $\times 10^7$ cm^2s^{-1} at the homopause and $\sim 10^5$ cm^2s^{-1} at the 1 millibar pressure level is obtained. Models with K varying approximately as the inverse square root of atmospheric number density, and those in which K rises steeply to 10^7 cm^2s^{-1} at ~ 0.1 mbar and then becomes constant with height, are equally valid for explaining the occultation light curves.

Bézard et al (1991) argue that a best fit to the IRIS C_2H_2 data is achieved by placing a stagnant region with K of 2×10^3 cm^2s^{-1} from the tropopause up to about 3 mbar, above which is a steep increase to 10^7 cm^2s^{-1}, constant above 0.1 mbar. However, Kostiuk et al (1992) argue that an eddy profile with 5×10^7 cm^2s^{-1} at the homopause and a downward decrease as roughly the inverse square root of the total number density fits the ethane data just as well. Additionally, the data are fitted just as well with a constant mixing ratio of ethane as a function of altitude, which would give no information on the value of K.

The need for a higher eddy diffusion in the Neptune stratosphere than in that of Uranus is a reasonably robust conclusion, supported also by UVS data on the Helium 584 Å emission line (Parkinson et al 1990); the possible desirability of a stagnant layer just above the tropopause is intriguing.

Further evidence for the nature of stratospheric mixing on these planets comes from the latitudinal variation of hydrocarbons. On Neptune the C_2H_2 emission observed using IRIS is lower at southern mid-latitudes than the equator (Bézard et al 1991). The effect cannot be correlated with the seasonal dependence of sunlight, and is more plausibly due to dynamical upwelling at mid-latitudes which lowers the temperature and hence the emission from the acetylene line. Alternatively, if the eddy mixing is more vigorous at mid-latitudes, it could have a direct effect on the acetylene abundance (Bézard et al 1991).

Recent work by McMillan & Strobel (1992), using the *Voyager* UVS

data set, indicates that at pressures below 1 millibar, methane, ethane, and acetylene are 10–100 times more abundant at the equator than at the poles. This variation is interpreted in terms of upwelling at low latitudes and subsidence near the poles. Since this is the pattern inferred for the troposphere from IRIS temperatures measurements (see below), it suggests that tropospheric circulation patterns penetrate into the stratosphere on Uranus. Finally, there is evidence from ground-based infrared observations that the strength of the ethane emission has varied from 1985 to 1991, which could be an indication of up to a 15% increase in ethane abundance during that time (Hammel et al 1992b) and hence of possible dynamical processes in the stratosphere.

Products of methane photolysis such as ethane, acetylene, and even heavier hydrocarbons have saturation vapor pressures that are much less than that of methane itself; hence these species all condense out in the lower stratosphere close to where saturation is achieved (Atreya & Ponthieu 1983, Atreya 1984, Romani & Atreya 1989, Moses et al 1992), forming a haze of aerosol particles which fall downward until they are eventually destroyed and the carbon recycled (see Figure 3). Evidence for stratospheric hazes is seen in *Voyager* Uranus data, and the photochemically produced higher-hydrocarbons can supply enough material to account for the haze optical depth (Pollack et al 1987), with the exception of very high altitudes (~ 10 μbar) where infalling dust may have to be invoked to explain extinction in *Voyager* photopolarimeter data (West et al 1987). The observed photochemical hazes are more absorbing in the visible part of the spectrum than would be expected for pure acetylene, ethane, and a third less abundant component, diacetylene (C_4H_2) (Pollack et al 1987), indicating that additional chemistry occurs to form heavy polymers in the aerosols, through the action of solar UV radiation and/or cosmic rays.

On Neptune *Voyager* photopolarimeter and imaging data show that the photochemical haze is, as on Uranus, optically thin but slightly ultraviolet-absorbing (Lane et al 1989, Smith et al 1989, Pryor, et al 1992). This implies again that while the primary haze production process is condensation of acetylene and ethane, some additional chemistry driven by UV or energetic particles produces a small fraction of dark, red heteropolymers in the haze (Khare et al 1987).

The abundance of minor species is important in understanding the bulk composition of these atmospheres as well. Recent submillimeter observations have detected both hydrogen cyanide (HCN) and carbon monoxide (CO) in the stratosphere of Neptune, with mixing ratios of 1.2×10^{-6} for CO and 1.0×10^{-9} for HCN (Marten et al 1993). These numbers are slightly higher than the determination of Rosenqvist et al (1992). HCN is

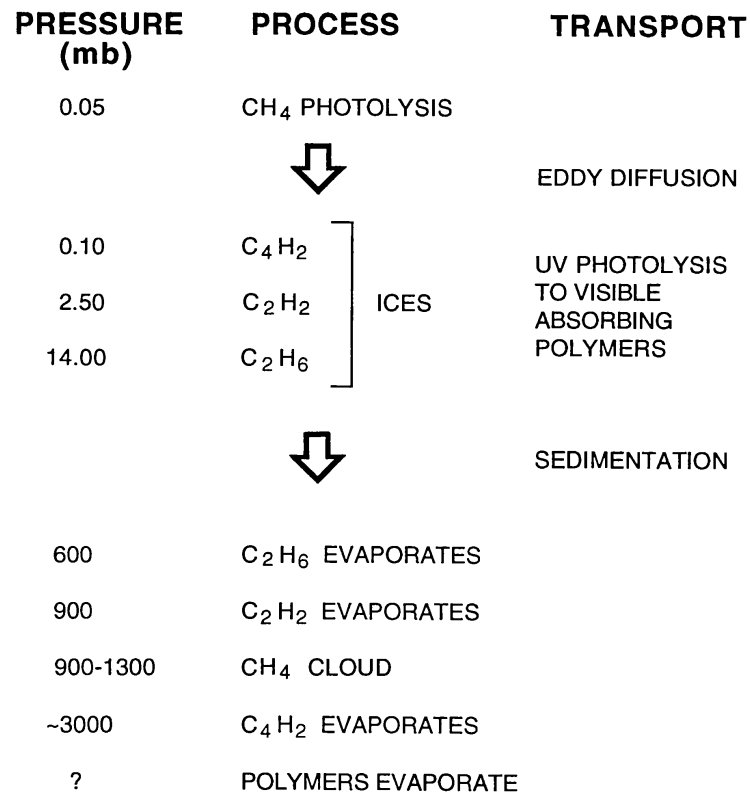

Figure 3 Schematic cycle of aerosol production and destruction, adapted from Pollack et al (1987). Pressure levels of ice formation refer to condensation, based on comparing gas-phase partial pressures of the species from a photochemical model with their saturation vapor pressures. Eddy diffusion refers to movement of gaseous species from their regions of production to condensation (with diacetylene also condensing out in its region of formation). Solar UV photons produce absorbing polymers in the aerosols. Pressure level of polymer destruction is uncertain because their composition is not well known.

likely to be produced photochemically with methane and molecular nitrogen (N_2) as the original parents. Molecular nitrogen is not the thermodynamically-preferred species in these hydrogen-rich atmospheres, but the time to convert it thermochemically to the primary stable species (ammonia) is much longer than the age of the solar system at stratospheric temperatures. Models favoring external supply, primarily from nitrogen atoms escaping off of Triton's atmosphere (Romani et al 1992), or internal supply, via rapid vertical mixing from deep hot regions where molecular nitrogen is more abundant (Marten et al 1993), are both possible.

The stratospheric CO abundance is far too high for thermochemical equilibrium in the observable atmosphere. However, the timescales for conversion to the primary stable species, methane, are again much longer than the age of the solar system as with nitrogen conversion. CO could be

supplied to the stratosphere by upwelling of gas from below: The large measured abundance suggests that catalytic reactions to equilibrate CO and CH_4 in the interior are inhibited (Marten et al 1993). If this explanation is correct, then molecular nitrogen also could be much more abundant then previously expected, perhaps competitive with or even dominating over ammonia depending upon the primordial mix of nitrogen-bearing species (Marten et al 1993). Evidence for ammonia in the observable atmosphere does exist, however, as discussed in the section on cloud structure. Alternatively, excess CO could be produced via water-bearing external sources such as icy meteoroids which ablate in the atmosphere, contributing oxygen (though the latter source may be too small; Moses 1992).

Energy and Opacity Sources

Given the compositions of the two atmospheres described above, the structure of the atmosphere can be understood in terms of opacity contributions from the various constituents and sources of energy present in the atmospheres. In the troposphere the predominant opacity source in the thermal infrared is collision-induced (also called pressure-induced) absorption by molecular hydrogen. This opacity source arises from collisions between molecules which distort the symmetric shape of the electron distribution of the hydrogen molecule, enabling the normally-forbidden dipole transition to take place. The dominant collision pair is H_2–H_2, but contributions to the shape of the spectrum from H_2–He and H_2–CH_4 are significant (Conrath et al 1991c). Unit optical depth due to this opacity source alone is reached at pressures below 0.5 bar (the upper troposphere) for wavenumbers from $< 100\ cm^{-1}$ to well above $800\ cm^{-1}$, encompassing the Planck function peak. The collision-induced absorption peaks at about $400\ cm^{-1}$, where unit optical depth is reached at 0.1 bar—roughly the tropopause (Conrath et al 1991c). In spite of the apparent simplicity of the atmospheric thermal balance arising from the predominance of the collision-induced hydrogen opacity source, in order to derive the helium abundance correctly from synthesized spectra as a function of temperature, high accuracy in the shape of the absorption is demanded. In consequence full quantum mechanical ab initio calculations for the three collision-pairs given above have been completed by Borysow et al (1985, 1988) and Borysow & Frommhold (1986).

At pressures exceeding 1 bar on both Uranus and Neptune the temperature gradient becomes very roughly constant, excepting a variation associated apparently with the base of the methane cloud in the 1–2 bar region (Lindal et al 1987, 1990). This constancy suggests that convection is carrying most of the flux at deeper levels. Application of the usual

Schwarzschild criterion (e.g. Clayton 1968) to determine whether the environmental (radiative) temperature profile exceeds the adiabat is hampered by the fact that the correct adiabat to use is dependent on the para- to ortho-hydrogen ratio as a function of altitude, and on the rate of exchange (i.e. degree to which equilibration is taking place) at each level. Different assumptions about the behavior of the para-hydrogen fraction with altitude lead to the two adiabats shown in Figure 4, either of which is consistent with the temperature gradient derived below the methane cloud on Uranus (Lindal et al 1987). In spite of this complication, it seems quite certain that convection becomes the predominant mode of upward energy transport at pressure levels below a bar or so.

The increase in temperature gradient with increasing depth, leading to

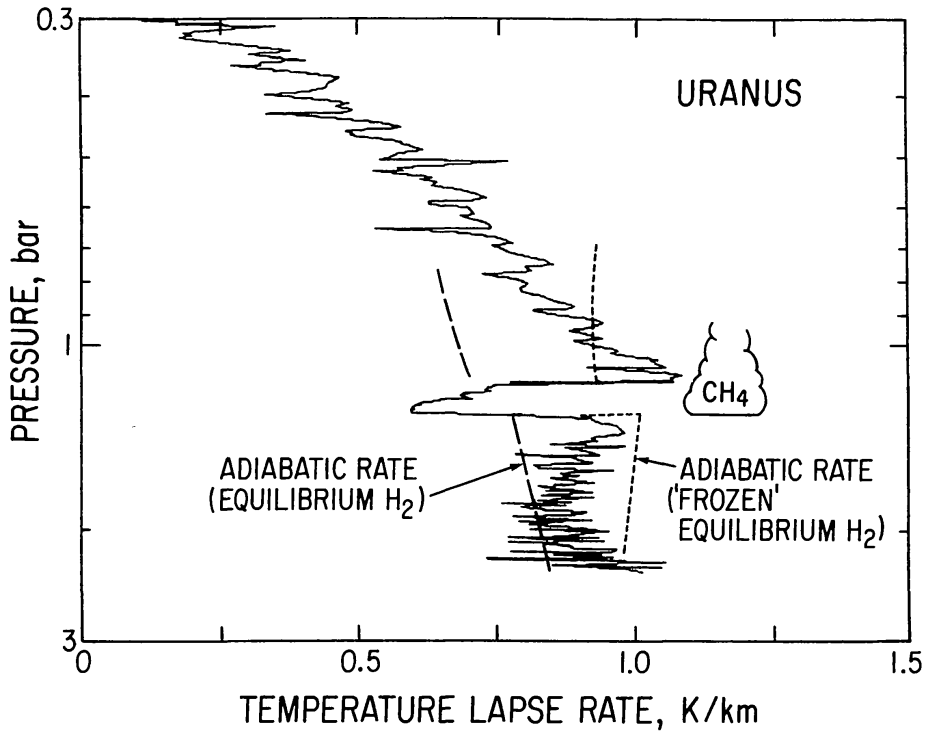

Figure 4 Plot of temperature gradient versus pressure in the Uranus troposphere, derived from the ingress *Voyager* radio occultation profile by Lindal et al (1987). The strong variation in the temperature gradient (actually a fluctuation in the refractivity data) is interpreted to be due to intercepting the base of a methane cloud, which is marked (the data do not say anything about the vertical extent of the cloud). For comparison, theoretical adiabats are shown for two cases. The dashed line corresponds to full equilibration at each temperature between para- and ortho-hydrogen; the dotted curve assumes that the para-hydrogen fraction is fixed or "frozen" at a value corresponding to the temperature at each level, but no interchange and hence no latent heat release occurs between levels. This frozen equilibrium model is described more fully in Gierasch & Conrath (1987), and in the text.

an apparently convective profile, is a standard signature of an atmosphere with a source of heat within or below the troposphere. In stars, the source of heat is deep-seated nuclear reactions or (for brown dwarfs) the virialized energy of collapse of the self-gravitating object. In the atmospheres of Venus, Earth, and Titan, sunlight transmitted more or less freely to the surface is thermalized at the ground (and to a lesser extent in the lower atmosphere), providing a surface heat flux which must be removed along a tropospheric temperature gradient. In the giant planets, both sunlight (thermalized in the troposphere) and internal heat supplied by initial collapse and subsequent differentiation drives convection.

Sunlight is deposited in the troposphere of Uranus primarily through absorption by methane in the 0.7 to 1.3 bar region, based on the radiative model of B. Bézard and D. Gautier (referenced in Conrath et al 1991b), which is tied directly to the *Voyager* radio occultation profile. This zone of deposition is largely determined by the steep vapor pressure dependence of methane on altitude, and is sufficiently narrow that it likely triggers dynamical processes to remove excess solar heating (Conrath et al 1991c). Although a similar model has not been constructed for Neptune, the earlier radiative-convective equilibrium models of Appleby (1986) indicate that there, too, methane is the predominant absorber of sunlight in the troposphere. The vertical distribution of the solar deposition is then dependent upon the vertical distribution of methane in the troposphere. Because methane may be oversaturated at the tropopause by an amount that remains poorly determined, and because the source of the oversaturation may involve vertical convective processes which could redistribute methane condensate throughout the upper troposphere (Lunine & Hunten 1989, Stoker & Toon 1989), the vertical distribution of solar heating in Neptune's troposphere must be characterized as highly uncertain.

Determination of the amount of energy coming through the troposphere from the deep interior requires accurate measurement of the bolometric thermal output of the planet, achieved most accurately using *Voyager* IRIS data, as well as determination of the amount of sunlight reflected and scattered by haze particles, which requires high phase-angle *Voyager* observations to complement the near-zero phase angle terrestrial observations (as described in Conrath et al 1989). Uncertainties arise largely because of the incomplete spectral and spatial coverage of *Voyager* instruments. The ratio of total heat flow (internal heat plus thermalized sunlight) to absorbed solar energy is 1.67 ± 0.09 for Jupiter, 1.78 ± 0.09 for Saturn, 1.06 ± 0.08 for Uranus, and 2.61 ± 0.28 for Neptune (Pearl & Conrath 1991). The lack of internal heat flow for Uranus relative to that for Neptune has little effect on the overall shape of the tropospheric temperature gradient, but results in nearly equal effective temperatures for the two bodies and hence

the absolute values of the temperatures versus altitude are much more similar than they would otherwise be (given the differing distances from the Sun). The implications of the very different internal heat flows for the styles of convection are discussed later.

In the stratosphere, absorption of sunlight is the primary source of energy, with upwelling from the troposphere being a secondary source of energy which transports tropospheric species into the stratosphere, as well as redistributes gases and heat latitudinally. On both Uranus and Neptune, the stratospheres are heated radiatively by CH_4 absorption of sunlight in bands at 1.7, 2.3, and 3.3 μm, as well as by aerosol absorption. On Uranus, the small stratospheric methane abundance, constrained by the low temperature of the tropopause, yields the rather shallow stratospheric temperature profile of Figure 1*b* and weak thermal emission (Orton et al 1990). The two bumps seen in the temperature profile of Figure 1*b* occur at pressure levels close to those at which C_2H_2 and C_2H_6 condense out, suggesting that discrete, thick aerosol layers may be responsible for the enhanced heating in those regions (Lindal et al 1987, Pollack et al 1987).

One difficulty with this notion is that pure ethane and acetylene haze lack the absorption coefficients at visible and near-UV wavelengths to absorb the requisite amount of sunlight (West et al 1991). As noted above, the continued photochemical processing of the haze to darker polymers alleviates this problem somewhat. Still, the required amount of absorption by aerosols above 0.5 bar is large (15% of the total solar energy received), and may not be compatible with the amount of sunlight observed to be reflected from Uranus, as noted by Conrath et al (1991c). These authors suggest that it is possible that additional sources of heating are required, for example, dynamical transport of heat from the poles to the equatorial latitudes of the radio occultation. (Since Uranus is "tipped on its side," the poles receive more sunlight than the equator on an annual average).

Neptune's stratospheric thermal emissions are much stronger than that of Uranus, and the corresponding stratospheric temperature gradient much steeper. The thermal emissions are so strong that models based on ground-based infrared observations such as described in Orton et al (1990) required very large amounts of methane, a mixing ratio of 2%, to warm the stratosphere adequately (Appleby 1986); aerosols cannot supply the heating for plausible abundances and spectral properties. This is the source of the requirement for a Neptunian stratosphere heavily oversaturated in methane. Bishop et al (1992) note that the ground-based data can be made to fit more closely their UVS-based determination of a smaller methane abundance on Neptune if the former are analyzed with a steeper stratospheric temperature gradient; however, full agreement requires an unreasonably warm stratosphere at 0.1 mbar. The Neptunian stratospheric

temperature profile shows no evidence for the hot layers seen in the Uranian middle stratosphere; since aerosols do form in the Neptune stratosphere, the lack of these features must be due to the overall steeper temperature gradient in the case of Neptune or a difference in the haze distribution and properties.

Cooling on both planets in the middle and upper stratosphere is primarily through emission by the acetylene band at 13.7 μm wavelength, as well as by the ethane band at roughly 12.2 μm; below the millibar level, hydrogen bands contribute (Conrath et al 1991c). Because of the low methane abundance in the Uranian stratosphere, cooling through the methane 7.7 μm band is negligible. If the methane abundance on Neptune is indeed significantly larger than saturation, cooling through this band must be important there, though the emission from this feature was not detected by IRIS owing to low instrument signal associated with the low temperatures (Bézard et al 1991). At pressure levels below 10 μbar, non-LTE (nonlocal thermodynamic equilibrium) effects in the methane vibrational bands have an important impact on the thermal structure, leading to variations in temperature (plus or minus) of as much as 20 K from the LTE models (Appleby 1986).

The temperature profile in the thermosphere of Uranus, shown in Figure 1*a*, rises to a surprisingly high exospheric temperature as determined from *Voyager* UVS data (Herbert et al 1987). The value for Neptune is also high but as yet uncertain (Broadfoot et al 1989), with analysis in progress, so we confine ourselves to the case of Uranus. Using a conductive temperature profile appropriate to the thermosphere, and thermal conductivity parameters for hydrogen, Herbert et al (1987) found a required thermospheric heating rate of $\sim$0.08 ergs $cm^{-2}s^{-1}$; the more recent analysis by Stevens et al (1993) finds 0.06 ergs $cm^{-2}s^{-1}$. The globally-averaged solar EUV input is 0.001 ergs $cm^{-2}s^{-1}$. Clearly another source of energy must be powering the thermal gradient in the thermosphere. Possible sources include: (*a*) "dayglow" (previously "electroglow"), in which low energy electrons dissociate molecular hydrogen, producing a flux of heat; (*b*) heating by production of aurora; and (*c*) joule heating induced as ions are constrained to move along magnetic field lines while the neutral gas is carried by upper atmosphere winds (Herbert et al 1987). The efficacy of dayglow is controversial as is the precise mechanism; this issue is tied to the surprisingly high ultraviolet emissions of the giant planets. This complex problem is ably reviewed in great detail by Strobel et al (1991). Radiation at the mesopause of heat conducted down from the thermosphere on both Uranus and Neptune is by hydrocarbon emission, with pressure-induced dipole and quadrupole hydrogen emission being relatively small (Strobel et al 1991).

Cloud Structure

The composition and thermal structures of the Uranian and Neptunian atmospheres imply the presence of condensation clouds at various levels of the troposphere. As noted above, microwave, infrared, and radio occultation measurements indicate somewhat more directly the presence of several types of clouds. Figure 5 from de Pater et al (1991) compares the location of clouds in the atmospheres of Uranus and Neptune, based on the inferred abundances of condensable species and the temperature profiles. In the case of a simple, one-component cloud, the base of the cloud will form at a level such that the partial pressure of the cloud forming constituent exceeds its saturation vapor pressure, which is a single-valued function of temperature. Although the gas may supercool slightly, so that condensation occurs at slightly colder levels than the precise level of saturation, this is a small effect in terms of the scale shown here (Moses et al 1992). For clouds which form of two components, i.e. where a minor species may go into solution in the cloud droplets of a more abundant constituent, or a chemical reaction takes place resulting in the production of a species of lower vapor pressure, the chemical potentials of each component in the vapor phase must be compared with its chemical potential in the condensed phase—where the latter becomes less than the former cloud formation will occur. Thus, computation of the vertical profile of cloud structure is achieved by computing an adiabatic temperature profile beginning below the deepest cloud of interest, and testing whether cloud formation is thermodynamically preferred at each level. Where clouds do form, the temperature profile is affected by the latent heat of condensation or reaction, and the amount of condensate at each level is limited by the saturation vapor pressure (a more detailed computation must take account of the fact that supersaturation as well as precipitation of condensate particles occurs). The temperature profile must merge with that determined by the *Voyager* radio occultation experiment (which probed to ~ 2 bars on Uranus and ~ 6 bars on Neptune).

de Pater et al (1991) assume a factor of 30 enhancement of CH_4 relative to solar (corresponding to the 2% mixing ratio inferred from the radio occultation cloud base in both planets), and sulfur enhanced by a factor of 10 relative to solar on Uranus and 30 on Neptune. Ammonia is assumed to be in solar abundance. Two alternative assumptions are made for water: solar abundance, and the same enhancement relative to solar as for sulfur. Moving upward from the base of each panel in Figure 5, liquid water clouds form at the deepest level in the observable atmosphere (less volatile constituents such as silicates and iron will form condensates much deeper still, but we do not consider these here). The water droplets contain a

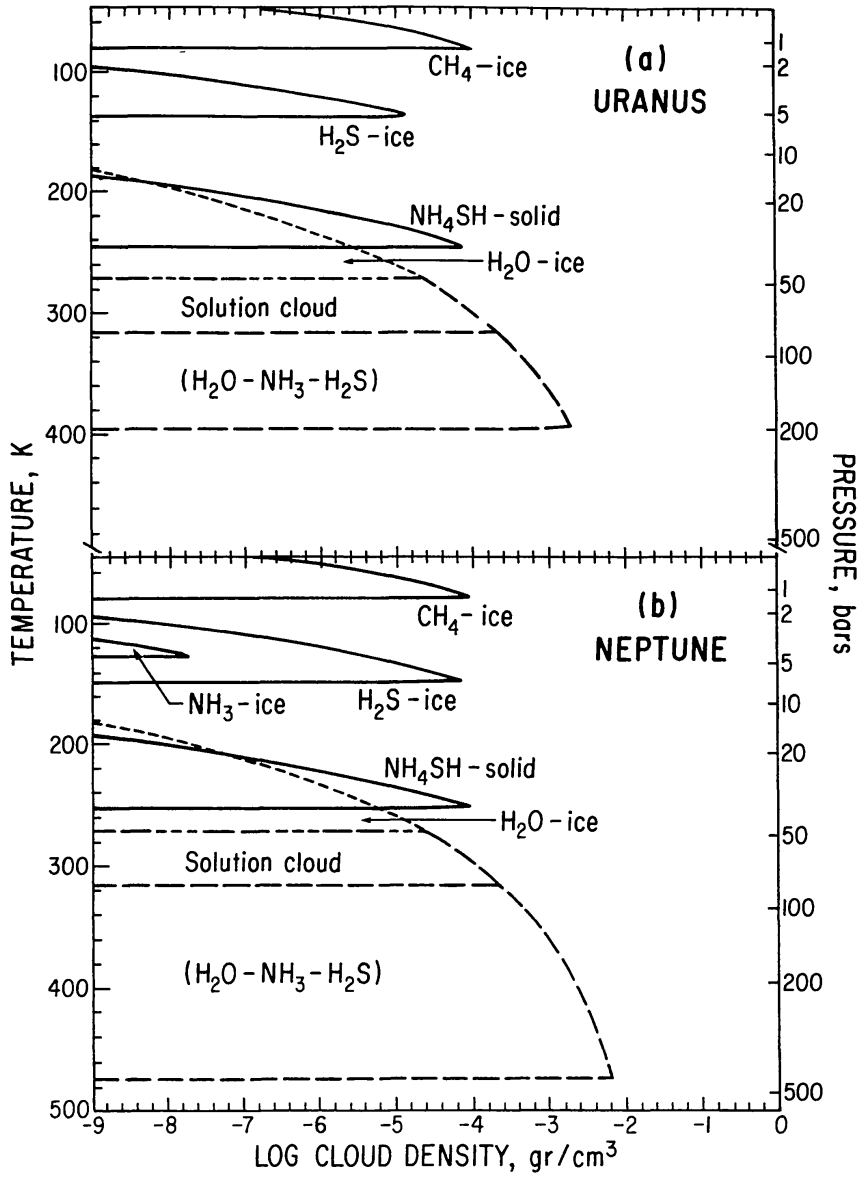

Figure 5 Vertical cloud structure in the atmospheres of (*a*) Uranus and (*b*) Neptune, plotted as pressure level versus number density of condensate, from de Pater et al (1991). Assumptions about the initial abundances of constituents and computational procedure are described in the text. The dashed curve is a liquid water cloud with ammonia and hydrogen sulfide as solutes; upper dashed cloud base assumes solar abundance of water below the cloud, and lower cloud base assumes an enhancement by a factor of 10 on Uranus and 30 on Neptune relative to solar.

significant fraction of ammonia and hydrogen sulfide (H_2S) in solution. The upper dashed cloud base corresponds to solar water abundance, the lower to the enhanced values. At 273 K the thermodynamically preferred water phase is ice, in which it is assumed the ammonia and hydrogen

sulfide are much less volatile. However the supercooling of liquid water droplets is likely to be significant, as it is on Earth, hence leading to liquid water drops several tens of degrees below the freezing point.

Just above the base of the water cloud, ammonium hydrosulfide is thermodynamically stable, and if the kinetics are sufficiently rapid, it will form. The hydrosulfide should remove most of the ammonia which would otherwise form a cloud at higher altitude. However, on Neptune the radio occultation data probe down to levels of 6 bars (Lindal et al 1990, Lindal 1992), where an increase in microwave opacity occurs corresponding to 6×10^{-7} mole fraction of ammonia, consistent with saturation over pure ammonia ice at the temperature of the 6-bar pressure level. While the opacity could be due to a sulfur compound, dePater et al (1991) argue that it is best attributed to ammonia (see below). Therefore, an ammonia cloud is shown in the 5-bar region on Neptune.

Although the radio occultation data do not reach this deep on Uranus, ground-based data indicate less opacity in the corresponding part of the Uranian atmosphere, suggesting that ammonia has been removed by a deeper hydrosulfide cloud. Therefore, an ammonia cloud is not shown for Uranus. The excess of sulfur over nitrogen assumed for this exercise based on fitting the deep microwave data (de Pater et al 1991) results in formation of a hydrogen sulfide cloud above the level of the ammonium hydrosulfide. Finally, methane condenses out at 1.2 bars on Uranus and 1.7 bars on Neptune in accord with the radio occultation results.

The presence of sufficient ammonia at 6 bars to make a cloud requires that the reaction $H_2S + NH_3 \Rightarrow NH_4SH$ not go to completion deeper down, because enough sulfur is available based upon the deep microwave observations (de Pater et al 1991) to remove most of the ammonia at that level. de Pater et al argue that since the reaction is heterogeneous (involves more than one gas species), it is likely to be slow unless solid particles, i.e. nucleation sites, are available in that region. If that pressure level has been swept clean of such particles by frequent rainout this explanation is plausible, though it needs quantitative evaluation.

Also at issue is why the same does not appear to be occurring on Uranus. One possibility is narrow layering: As discussed below, the temperature gradient profile in the Uranian troposphere shown in Figure 4 and the para-hydrogen fraction inferred from *Voyager* data can be reconciled if it is assumed that convection in the 1-bar region occurs in very narrow layers, stabilized perhaps by molecular weight gradients. (Recall that in contrast to the Earth, all condensing gases on Uranus and Neptune have molecular weights larger than the mean molecular weight of the background gas, hydrogen-helium.) Such layering might occur as well in the 20-bar region and below, where significant condensation is occurring and the cor-

responding molecular weight gradients are also large and stabilizing. Such layers would be thermally conductive but effectively impermeable to gases (Gierasch & Conrath 1987), allowing for a long dwell time for the ammonia and hydrogen sulfide in an environment in which the hydrosulfide is thermodynamically stable. This would encourage equilibration of the hydrosulfide reaction. One then might ask why the same does not occur on Neptune, and one possibility is that the vastly larger internal heat flux of Neptune (compared to Uranus) tends to encourage strong, rapid vertical upwelling which discourages thin layering. In a sense the process is self-reinforcing: Strong upwelling leads to disequilibrium, preventing formation of the sulfide cloud and hence mitigating against formation of stabilizing molecular weight gradients. The lack of a strong thermal emission signature on Uranus over and above thermalized sunlight is consistent with the notion of narrowly-layered convection taking place.

While the basic method of computation of the vertical cloud structure presented above is standard, specific results vary depending upon assumptions about the chemical equilibrium constants, treatment of the temperature profile, etc. Carlson et al (1987) derive qualitatively similar results to that of de Pater et al (1991), though with a different estimate of the enhancement of sulfur required to explain the apparent depletion of ammonia from the microwave data. Generally, more recent cloud models in the literature represent refinements and improvements over earlier models.

The global appearances of the two atmospheres can be correlated with the cloud model presented above. The general blue color of the two bodies has been ascribed to gaseous methane absorption preferentially in the red part of the spectrum. However, at least for Neptune, Baines & Hammel (1992) argue that the absorption of red light is occurring primarily in the background, (mostly) hydrogen sulfide cloud. Rayleigh scattering in the gas is also important in making deeper features appear darker (Smith et al 1989); high clouds will appear bright against the disk. Some of these features have sufficient contrast to be detected with ground-based telescopes, and were known prior to the *Voyager* encounter (Hammel 1989). The Neptune atmosphere shows a variety of light and dark features in *Voyager* images which can be tracked in their zonal (east-west) movement around the planet. High phase angle images, including one which shows shadows of bright cloud features against the background cloud, allow determination of the altitude of the bright features above the background cloud which are found to be in the range 50–150 km (Smith et al 1989). If the background cloud tops are at roughly the 3-bar level, as seems to be case from ground-based studies of methane and hydrogen absorption features (Baines & Smith 1990), then the bright features are at pressure

levels 2 to 5 scale heights higher. This picture is roughly consistent with the notion that the background cloud is hydrogen sulfide, and ammonia (see Figure 5) with methane clouds forming at 1.5 bar and extending (as cloud tops or sheared-off material) up to (or through) the tropopause. Darker regions of the visible surface could be interpreted as holes in the hydrogen sulfide cloud material through which one is seeing deeper (Smith et al 1989). Bright cloud features which have high spatial and temporal variability are seen against the dark regions, suggestive of the bright tops of upwelling convective columns. Other bright, and hence high altitude clouds appear to be sheared along the margins of oval dark regions (such as the Great Dark Spot, crudely akin in appearance to Jupiter's Great Red Spot) and along the margins of regions of differing zonal flow. The general impression from the *Voyager* images is of an atmosphere with strong zonal flow (shown by the banded structure in the background clouds) against which regions of strong vertical upwelling are carrying cloud material to great heights, where the material ceases to rise and is sheared by the general flow. Limb images confirm the presence of photochemically-produced stratospheric hazes.

Uranus, on the other hand, shows little contrast in its atmosphere, with variations from latitude to latitude of 5% at optical wavelengths. Some (nonphotographic) ground-based observations hint at zonal motions (see Allison et al 1991 for a discussion), but only a few features that can be tracked appear in *Voyager* images. The rarity of bright plumes and other discrete features gives the impression of an atmosphere where substantial vertical motions are suppressed. Limb and polar brightening on Uranus, particularly in the near-infrared where methane absorbs strongly, suggest one is seeing stratospheric hazes in the atmosphere (Allison et al 1991); however, as noted above, these hazes are optically thin and hence are not obscuring details in the atmosphere beneath.

Baines & Bergstralh (1986), with revisions as described in West et al (1991), have derived the optical thickness and pressure at the top of the methane cloud on Uranus from molecular hydrogen bands and methane bands in the optical and near-infrared, measured from the ground. They find that the cloud optical depth is in the range 0.3 to 0.9 with the cloud top at 2.4 to 3.4 bars. Referring to Figure 5 suggests that the derived cloud-top pressure is somewhat too large (i.e. the cloud is too deep).

Observations of limb darkening at 6190 Å (Rages & Pollack 1988) provide an additional constraint on the methane cloud optical depth of 0.2 and location of the cloud of around 1 bar at low latitudes. This is in much better agreement with the cloud model based on *Voyager*-derived methane abundance. Subsequent reanalysis of the methane observations using new low-temperature absorption coefficients for methane at 6190 Å

(Smith et al 1990) yield a pressure for the top of the lower cloud (the presumably H_2S cloud below the methane cloud) of about 2.4 bars, which forces the methane cloud base to move up and be in better agreement with *Voyager* data. The reanalysis illustrates the danger of using room temperature absorption coefficients for methane, as in previous studies, and the necessity of measuring the low temperature absorption coefficients—a difficult task.

Both atmospheres show evidence for variability in appearance over time. Ground-based observations of Uranus suggest an increase in brightness at visible wavelengths from 1972–1981 (Lockwood et al 1983). Lockwood et al proposed that the polar region, which was then coming into view as seen from the Earth, was brighter than the equator. The required contrast between hemispheres is 14% for such an effect to produce the 7% change seen at blue wavelengths (West et al 1991), and is in conflict with *Voyager* and balloon-borne measurements of the contrast. Therefore, either systematic errors in calibration, or a temporal variation, caused the brightening. Sudden brightening events on Neptune have been observed at least since the mid-1970s (Joyce et al 1977). A general brightening beginning in 1985 (Lockwood et al 1991) is reported. By observing in broadband blue and yellow filters, as well as in the methane 8900 Å band, Hammel et al (1992a) were able to interpret the brightening in terms of an increased production of bright regions on the surface, which by inference were methane clouds driven to high altitudes. By constructing rotational light curves, Hammel et al (1992a) determined that a single discrete feature was the initial source of the brightening, but that the bright material spread to other longitudes over time. Neptune's appearance returned to pre-1985 levels by 1989–1990 (Hammel et al 1992a), suggesting that the atmosphere is capable of a higher level of activity than that imaged by the *Voyager 2* cameras.

Horizontal Structure of the Atmospheres

Heretofore we have considered the thermal structure in the one-dimensional, vertical sense; variations across latitude ("meridional") and longitude ("zonal") are of high interest as well. The key *Voyager* data sets to infer horizontal structure are the radio occultation temperature profiles, spatial mapping of atmospheric temperatures by the IRIS experiment, and tracking of cloud features.

Circulation patterns at the tops of the visible clouds provide an important constraint on the atmospheric dynamics. Unfortunately, few such features exist on Uranus, but those that do exist indicate prograde winds of 150 meters per second at midlatitudes, declining toward the equator (Allison et al 1991). Here prograde means winds that move in the direction

of the planet's rotation, and hence have drift periods shorter than the rotation period of the planet. The rotation period of the planet, i.e. of its bulk interior, is assumed to be given by the rotation rate of the magnetic field as measured from *Voyager* particles and fields experiments. The radio occultation experiment relies on very precise measurement of the difference in distance of two surfaces at constant pressure from the center point of the occultation (Lindal et al 1987); these observations imply a wind speed near the equator that is *retrograde* at about 100 m s^{-1}. The radio occultation result is averaged over the region probed by the experiment with good signal to noise, but crudely can be assumed centered at about 1 bar. Since the visible cloud features are also roughly at this level (assuming they are condensed methane) one can correlate the optical tracking of cloud features at high to mid-latitudes with the equatorial determination from the radio experiment.

On Neptune, the very high contrast atmosphere provided ample cloud features which could be tracked through images. The overall pattern is prograde rotation at high latitudes, transitioning to retrograde rotation at mid- to low latitudes (Limaye & Sromovsky 1991). The wind speeds are generally comparable to those found at Uranus, with the exception of the presence of a narrow, high speed (300 m s^{-1}) jet at 70°S latitude on Neptune. The radio occultation ingress measurement could be used to estimate a wind velocity by a slightly different technique than that employed for the dual ingress-egress measurements at Uranus (Lindal et al 1987, 1990). This yields a 170 m s^{-1} prograde wind near 60°N and a 6-bar pressure level. Other than the narrow jet, Neptune's cloud-top wind profile differs qualitatively from that of Uranus in having a retrograde region that extends to higher latitudes from the equator. By a fit of the gravitational figure of the planet, Hubbard et al (1991) deduced that the differential zonal flow on Neptune is a skin effect, rather than part of a deep-seated differential flow (e.g. rotation on cylinders).

The IRIS experiment yielded temperature versus latitude at various altitudes in the Uranian atmosphere. Flasar et al (1987) binned these data into pressure regimes corresponding to the tropopause region (60–200 mbar), and the troposphere above the base of the methane cloud (0.5–1 bar), as shown in Figure 6*a*. The temperature is a maximum near the equator, exhibits minima at mid-latitudes (most strongly in the south), and then rises toward the poles. The effect is much more pronounced in the higher altitude region, and is nearly absent at altitudes below the 500 millibar pressure level. The horizontal temperature structure in the stratosphere is, to first order, radiatively controlled, with a substantial phase lag relative to solar insolation owing to the long radiative time constant.

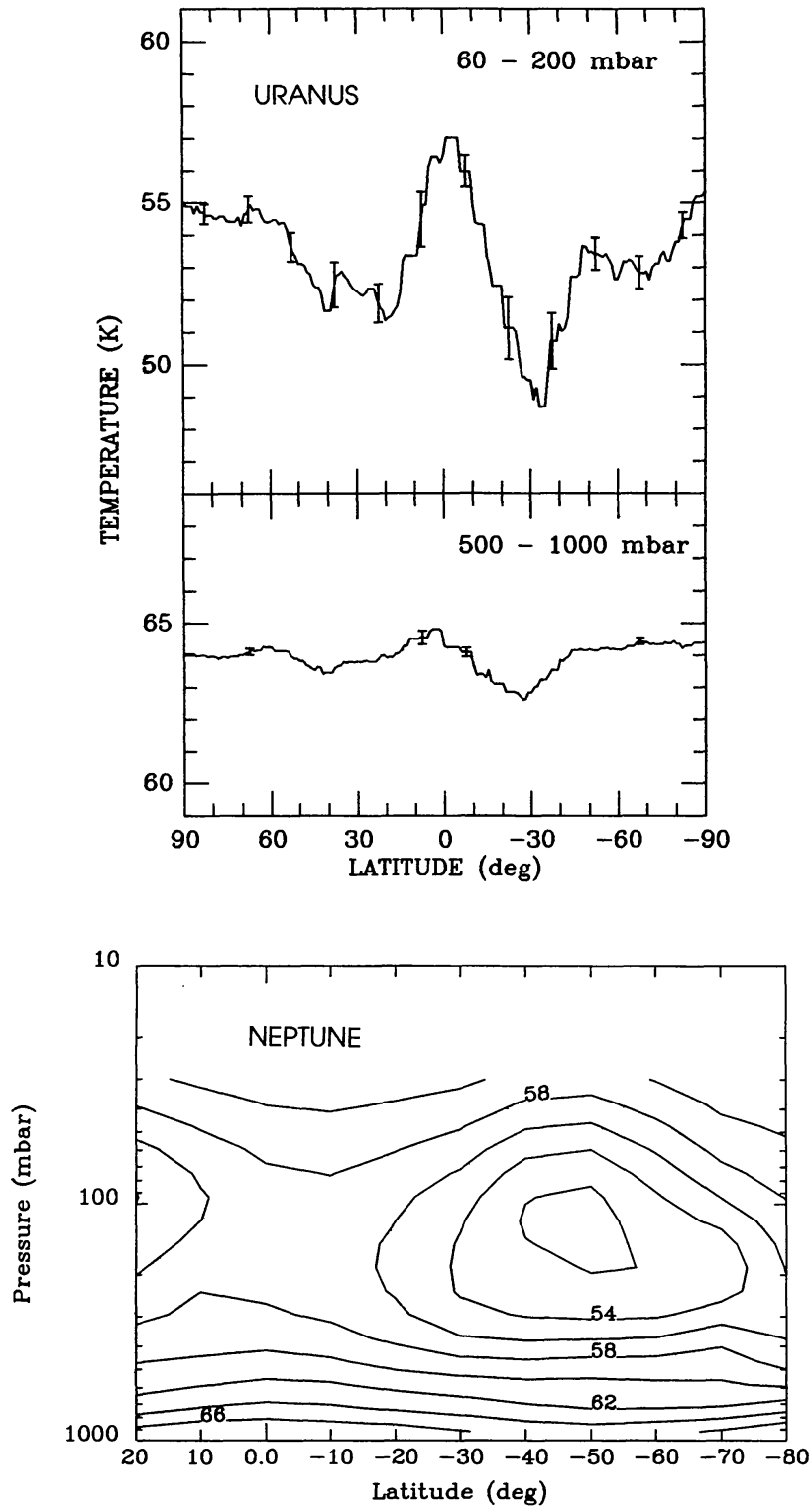

Figure 6 Temperature versus latitude on Uranus and Neptune from *Voyager* IRIS data. (*a*) For Uranus, temperature versus latitude is shown for two broad altitude regions, from Flasar et al (1987). (*b*) A contour map shows latitudinal temperature as a function of pressure level (in millibars) in the atmosphere of Neptune, from Conrath et al (1991a).

The cold anomalies at mid-latitudes on Uranus, defined somewhat more sharply in the south, are of particular interest. Although Smith et al (1986) proposed that the region was cold because of a lack of methane cloud condensation and hence latent heat contribution, the deep (>2 scale height) nature of the anomaly makes this explanation unlikely. Instead, the interpretation of Figure 7, from Flasar et al (1987), is much more plausible: upwelling in the region causing adiabatic cooling, with subsidence at adjacent latitudes leading to heating. An estimate of the vertical upwelling velocity can be obtained from a model in which the pressure scale height is the relevant length scale: A vertical velocity of order 10^{-3}–10^{-4} cm s^{-1} is obtained (Flasar et al 1987). This is much smaller than the vertical velocities achievable on Neptune associated with cloud condensation (moist convection) which we consider later.

Assuming that this atmosphere is in hydrostatic equilibrium, that the Coriolis force balances the pressure gradients ("geostrophic balance"), and that the ideal gas law applies, we can relate the latitudinal temperature gradients to the zonal wind speed U:

$$\frac{\partial U}{\partial \phi} = -\frac{R}{fa}\frac{\partial T}{\partial \Lambda}. \qquad 2.$$

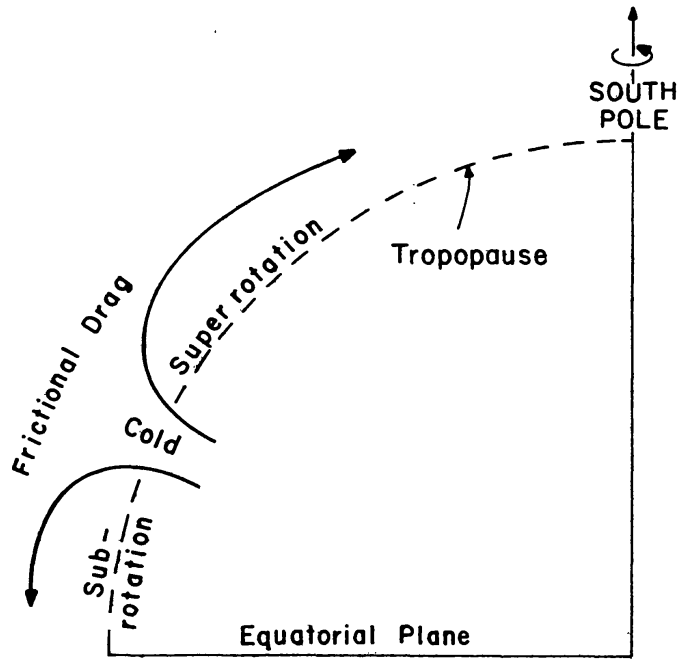

Figure 7 Model of meridional circulation pattern and consequent zonal wind directions in the southern hemisphere of Uranus, from Flasar et al (1987). A similar pattern is assumed for the northern hemisphere. Data for Neptune are consistent with a similar pattern.

Here ϕ is $\ln(p_o/p)$, a vertical coordinate in log-pressure space, R is the gas constant, a is the radius of the planet, and T the temperature. The parameter $f = 2\Omega\sin\Lambda$, where Ω is the angular rotation rate and Λ the latitude (Allison et al 1991). Additional conditions under which use of this "thermal wind" equation is valid are given in Allison et al (1991).

The resulting wind shears in the two altitude bins on Uranus are given in Flasar et al (1987); they can be converted to a meridional wind profile using a model. Flasar et al (1987) considered a model in which the tendency of the zonal flow to accelerate (due to conservation of angular momentum in parcels of air moving meridionally) is balanced by frictional damping. The model yielded a good fit to the cloud-top wind velocities derived from *Voyager* data, when the strength of the frictional damping was adjusted to fit the horizontal temperature profile. The essence of the model, then, is that the meridional wind structure on Uranus is consistent with a very weak, slow circulation characterized by upwelling at mid-latitudes, and damping by friction. The source of friction is open to speculation: Flasar et al (1987) suggested that gravity waves (vertically propagating oscillations in density and temperature in a stably stratified atmosphere) might break in the stratosphere, leading to dissipation. Furthermore, the latitudinal distribution of hydrocarbons in the middle stratosphere is crudely consistent with the circulation pattern shown in Figure 7 (McMillan & Strobel 1992).

The model presented above does not address the origin deep down in the atmosphere of the meridional circulation and zonal winds. The literature addressing the origin of zonal circulation on the giant planets is large. Of note for Uranus is the model of Friedson & Ingersoll (1987). They found that the low internal energy flux for Uranus is significant, in that it tends to force the observable atmosphere to transport most of the meridional heat by eddy processes. A stronger internal heat source would tend to allow heat to be transported toward the poles by deeper thermally-driven motions. However, the large obliquity of Uranus leads to a bimodal, seasonal behavior of the meridional energy balance, such that during equinox, one of the sunlit hemispheres could exhibit changes in the internal heat flux associated with (diurnally-averaged) meridional variations in solar heating (Friedson & Ingersoll 1987). This might be difficult to measure directly, but could lead to a different behavior of cloud motions and activity between the hemispheres. *Voyager 2* flew past Uranus during solstice, when any hemispherical variations in appearance could not be measured, since one hemisphere was in darkness. Detection of such effects would require either a spacecraft mission to Uranus during the coming equinox, twenty years hence, or use of ultrahigh resolution telescopes.

For Neptune the horizontal temperature structure is qualitatively similar

to that of Uranus, as shown in Figure 6*b* from Conrath et al (1991a). In this analysis, the IRIS spectra were used to generate altitude profiles, rather than binned into two altitude regimes. There is a slight asymmetry in the temperature distribution with respect to the equator, which does not fit a seasonal variation but instead may represent a perturbation due to the Great Dark Spot. A very recent derivation of the thermal wind gradient from Equation 2 and the thermal winds from the linear friction analysis described above yields a reasonably good fit to the cloud-top wind data, using a frictional damping constant similar to that for Uranus (Conrath et al 1991a). Hence the Neptune data are consistent with a rather sluggish circulation pattern near the tropopause akin to that of Uranus, in spite of the obliquity and internal heat flow differences.

TWO CURRENT OUTSTANDING PROBLEMS

The overview of the atmospheres of Uranus and Neptune given above identified a number of key areas in which considerable uncertainty exists at present, and which involve rather significant issues about the basic workings of these atmospheres. We consider here in somewhat more detail a subset of the problems. We focus on (*a*) the nature and implications of the different internal heat flows on the two planets; and (*b*) the implications of the deuterium and helium abundances for the origin and evolution of these ice giants, as distinct from Jupiter and Saturn. The discussion relies on the information presented above; hence reference to the literature will be less complete in what follows.

Energy and Mass Transport in the Tropospheres of Uranus and Neptune

The significantly disparate internal heat flows measured for the two planets, if indeed representative of the temporal and spatial average of the internal heat flux, imply that most of the heat being transported through the observable atmosphere is derived from energy sources deep in the interior on Neptune, whereas on Uranus, if any such source of energy exists, the atmosphere is transporting little or none of it outward. The origin of this difference in the formation or present internal structures of the planets has been considered (for example, Hubbard 1978), but remains poorly understood. Nor is there consensus on what the differing internal heatflows mean for the mechanisms of energy transport in the troposphere. The assertion explored in this section is that there are a number of observations, or inferences therefrom, which support the notion that strong vertical mixing in the troposphere is a more important energy and mass transport mechanism on Neptune than on Uranus. These observations are

listed below, in order of altitude from the top of the atmosphere down, with rough pressure levels indicated:

1. ($P < 0.1$ bar) The eddy mixing coefficient appears greatly enhanced in the Neptunian stratosphere relative to that of Uranus. (This is not necessarily connected to tropospheric processes, but we list it here because it becomes relevant in our later discussion of moist convection).
2. (10^{-6} bar $< P < 0.1$ bar) The abundance of methane is generally larger in the lower stratosphere of Neptune than that of Uranus, and in Neptune may be oversaturated by as much as a factor of 100 relative to the abundance permitted by the temperature minimum at the tropopause. This suggests strong vertical motions are required to move methane condensate through the tropopause region.
3. ($0.01 < P < 1$ bar) Fitting of *Voyager* IRIS spectra to derive a helium abundance on Neptune requires a methane cloud optical thickness in the infrared in excess of 1–2, which translates into visible optical depths inconsistent with imaging and other optical data. (An alternative model, which uses a stratospheric haze of optical depth 0.2–0.8, is also inconsistent with data in the visible part of the spectrum). Conrath et al (1991b) suggested that a reconciliation can be achieved if horizontal heterogeneity is imposed on the methane clouds, specifically "thick cumulus towers covering some fraction of the field of view in an otherwise clear atmosphere." Cumulus towers on Earth are signatures of strong vertical motion. The resulting fits also require particles larger than $\sim$one micron, suggestive of particle growth (and hence vertical convection). On Uranus, cloud models are not invoked to fit the IRIS spectra. However, a low methane vapor abundance in the upper troposphere, consistent with relative humidities (i.e. the ratio of the methane pressure to its saturated value at each temperature) of less than 50%, does seem to be required to match the IRIS spectra and radio science data for Uranus adequately (Conrath et al 1987).
4. ($0.1 < P < 3$ bars) The visible appearance of the Neptunian atmosphere is characterized by numerous high clouds, some of which may be in the lower stratosphere, which are likely to be methane condensation clouds originating at the 1-bar pressure level. Some of the cloud features that have not been sheared by zonal flow appear very similar to the tops of deep convective cells, and are time variable on a scale of hours.
5. (3 bars $< P < 30$ bars) Evidence exists from the radio occultation data, of an ammonia-ice cloud in the 5-bar region of Neptune (where hydrogen sulfide clouds also form). This is inconsistent with the simultaneous assumptions of thermodynamic equilibrium and enhanced sulfur-to-nitrogen ratio required to explain the microwave results

deeper in the atmosphere, because the enhanced sulfur would remove essentially all of the ammonia from the atmosphere as NH_4SH well below the 5-bar region. Inhibition of hydrosulfide formation at 20 bars requires lack of condensation nuclei and/or efficient vertical transport of ammonia through the 20–30 bar region (Figure 5). Lack of evidence for a high ammonia cloud on Uranus suggests that equilibrium between the gas and condensed phases is achieved in the deep ammonium hydrosulfide cloud.

6. (P $\sim$ kilobars) The detection of carbon monoxide in the atmosphere of Neptune at the part per million level (Marten et al 1993) potentially constrains the rate of mixing deep in the Neptunian atmosphere. If the CO is of internal origin (i.e. derived from thermochemical reactions) as opposed to added externally or by photochemistry), then a part per million is chemically stable at about 1200 K and several tens of kilobars pressure (Fegley & Prinn 1986). To mix the CO upwards through cooler but still chemically active regions (where conversion to methane reduces the CO abundance) to the observable atmosphere requires very rapid vertical mixing and perhaps inhibition of grain catalysis (Marten et al 1993). This picture is inconsistent with a thin stable layering model for Neptune. The upper limit on Uranian CO is 30 parts per billion (Marten et al 1993), which is not yet well-enough constrained to rule out substantial vertical mixing; an upper limit much less than a part per billion would be required. Molecular nitrogen is a similar chemical probe, and the detection of HCN in the atmosphere of Neptune but not Uranus is consistent with vigorous upwelling of N_2 in the former but not in the latter. If CO and HCN on Neptune are of external origin, however, they do not provide a constraint on deep tropospheric mixing.

Lines of evidence that are uncertain because of lack of comparable data on both bodies, or that argue against significant differences in tropospheric energy and mass transport on the two bodies, include:

1. ($P > 1$ bar) Reference to Figure 4 shows that the temperature gradient in the Uranus atmosphere is consistent with a "frozen" para-hydrogen fraction just above the methane cloud base, and is intermediate between the frozen and fully equilibrating gradients below the cloud base. At the same time, however, the para-hydrogen fraction appears to be equilibrated near the 900 mbar level based on *Voyager* IRIS data (Hanel et al 1986). Gierasch & Conrath (1987) argue that these two observations are best reconciled if convection occurs in narrow layers below the cloud base; within each layer, para-ortho equilibration is achieved but material is limited to each narrow layer so that vertical exchange of latent heat associated with the equilibration does not occur.

While the radio occultation analysis for Neptune is not as far along as for Uranus, recent ground-based and *IUE* measurements suggest that the para-hydrogen fraction on Neptune corresponds to the equilibrium state (Baines & Smith 1990). It will be of great interest to determine as accurately as possible the temperature gradient in the Neptunian troposphere so as to assess whether (as for Uranus) it is consistent with a "frozen equilibrium" profile. An important caveat with regard to Uranus is that ground-based data do not fully support the notion that para- and ortho-hydrogen are in equilibrium in the troposphere. Baines & Bergstralh (1986), from reflectance data, find that the fraction of hydrogen in the equilibrium state is between 0.63 and 0.95, somewhat below the 900 mbar region; far-infrared/submillimeter data (Orton et al 1986) yield a para-hydrogen fraction closer to the frozen value, in the 1–6 bar region, for a methane abundance of 2%.

2. The overall meridional flow on both Uranus and Neptune is characterized by rather slow upwelling at mid-latitudes, in spite of the different internal energies and seasonal insolation patterns. The Friedson & Ingersoll (1987) model suggests that internal energy on Uranus may be shunted meridionally in response to the modulation of solar heating associated with the seasons. Therefore, the energy balance analysis and particularly the bland appearance of Uranus may not apply in a time-averaged sense.

Perhaps the most observationally-accessible aspect of this problem is the methane abundance. While estimates for the Neptunian value in the stratosphere have decreased based on recent work, it still appears that this value exceeds that on Uranus. Two attempts to understand this difference quantitatively, in terms of vigorous convective plume activity in the troposphere (Lunine & Hunten 1989, Stoker & Toon 1989) yield insights into the possible processes occurring at these altitudes which are worth examining in some detail.

Following a suggestion by Hunten (1974) that methane might be carried through the tropopause by convective penetration, Lunine & Hunten (1989; hereafter LH) and Stoker & Toon (1989; hereafter ST) examined conditions under which condensation of an uplifted methane parcel could initiate sustained buoyant upwelling, or "moist convection," using the terrestrial meteorological term for cumulus/cumulonimbus formation. On Earth, the condensable water vapor is lower in molecular weight than the nitrogen-oxygen background mixture. Hence an upwelling cloud column ("plume") which is saturated in water vapor, rising through an environment of sinking, undersaturated air (the usual terrestrial situation), will be buoyant for two reasons: (*a*) the latent heat released as water condenses

during uplift contributes heat and hence buoyancy to the plume; (*b*) the air in the plume contains more water vapor than the outside ambient air; under the condition of pressure equilibrium between the two parcels the plume air is lighter and hence buoyant. In the giant planets, however, the condensable always has a molecular weight larger than the background gas, so that (*a*) and (*b*) work in opposite senses. Therefore, it is harder or impossible to propagate plumes in the giant planet atmospheres under conditions that would be favorable on Earth.

LH and ST used a simple one-dimensional momentum balance model for a plume developed originally by Hess (1979) and first applied to the giant planets by Stoker (1986). Imagine a parcel of moist air rising adiabatically within a specified background environment. The buoyancy force on a parcel of condensing air is computed as the fractional difference between the "virtual temperature" of the parcel and the environment. The virtual temperature is just the temperature of dry (without condensable gas) air with a density equal to that of moist air at the same pressure. Thus the effect of molecular weight differences between the plume and the environment is embodied directly in the virtual temperature. The temperature gradient in the plume is given by an adiabat corrected for the heat release associated with the latent heat of condensation. The latent heat effect tends to raise the virtual temperature relative to a parcel in which condensation does not occur. For a specified background temperature gradient (which is normally imposed by observations, e.g. the radio occultation profiles), the buoyancy of a parcel at each altitude is thus determined through the difference in virtual temperatures: The parcel is buoyant if its virtual temperature is larger than that of the environment. Given a buoyancy at each altitude, conservation of momentum then yields the parcel's upward (or downward) velocity at each level. Finally, the model must account for the entrainment of dry air into the moist, rising column. For the one-dimensional plume, this is done in a parameterized fashion: The amount of entrainment per altitude bin is inversely proportional to the diameter of the plume, i.e. it is a function of the ratio of the surface area to volume of the plume. The equation set used in the model may be found in Hess (1979), Stoker (1986) and LH.

LH examined conditions under which moist convection may take place, under the assumption that, like the Earth, the rising column is saturated: (*a*) the environmental temperature gradient must be adiabatic or slightly steeper than adiabatic; (*b*) the surrounding environmental air must be fully saturated in methane; (*c*) the moist parcel must be uplifted a significant fraction of a scale height beyond the cloud base before buoyant upwelling is initiated, or alternatively, the parcel must supersaturate by a significant factor (i.e. condensation must be delayed until the vapor pressure is larger

than the saturation value) for positive buoyancy to be initiated right at the condensation level.

LH examined particle growth timescales in the upwelling cloud and concluded that updraft velocities were sufficiently vigorous that a significant fraction of the condensate could be lofted into the stratosphere. Once above the tropopause, particles must be carried upward (meaning, for the stratosphere, towards higher temperatures) to a level where they will sublime and hence contribute to an enhanced methane mixing ratio in the gas phase.

A critical examination of each of the assumptions and requirements presented above is instructive in understanding whether this type of moist convection could enhance the Neptunian stratosphere in methane. The requirements on the environmental temperature profile are explored more fully in ST. In the case where the condensable gas is heavier than the background, the criteria are complicated. The dry adiabatic temperature gradient (temperature drop per altitude) $\Gamma_D = g/c_p$, where c_p is the specific heat at constant pressure. Figure 8 from ST illustrates that as one moves from an environmental lapse rate that is isothermal to one that is fully adiabatic, the condensing plume goes from fully buoyant to neutrally stable (at $\Gamma_D/2$) to negatively buoyant at the base, transitioning to positive buoyancy (at Γ_D). Since the *Voyager* data show the temperature profile to be nearly adiabatic on both Uranus and Neptune, the relevant part of the figure lies close to the dry adiabat. There the amount of uplift required for positive buoyancy and the vigor of the plume become sensitive functions of whether the environment is slightly sub- or superadiabatic. The measured temperature profile on Uranus in the convective zone appears to be affected by the presence of the methane cloud base and by the small or zero amount of para-ortho transitions below the base. Neither LH or ST incorporated the effects of para-ortho equilibration into their models, but these may be important, both in altering the background temperature profile and in contributing some latent heat in the plume. Also, the Neptune radio occultation data have not been analyzed to the same level of detail as those for Uranus, so that a detailed comparison between the two with regard to the effects on moist convection is premature.

Requirement (*b*), that the environment be saturated in methane, is required to overcome the molecular weight penalty associated with methane. LH argue that if indeed the Neptune stratosphere were very oversaturated in methane, the air subsiding back into the troposphere would contain large amounts of methane and provide significant relative humidity in the upper troposphere. Such a situation might be self-sustaining in that the heavy sinking air would continue to encourage the moist convective pumping of methane into the stratosphere on Neptune. On Uranus, the

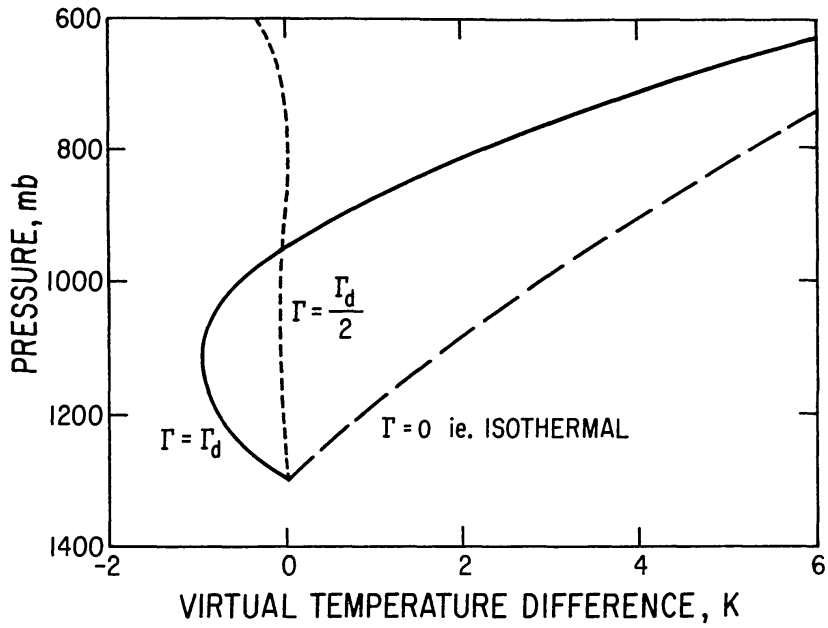

Figure 8 Buoyancy of a methane-saturated parcel versus pressure level, from ST. The buoyancy is positive for a positive virtual temperature difference. The three curves correspond to three different values of the environmental temperature gradient, expressed as a fraction of the dry adiabat Γ_D.

small amount of stratospheric methane implies that sinking air is dry, discouraging moist convection from occurring and hence reinforcing the existing situation.

One issue raised by this picture, however, is whether the stratosphere and subsiding regions of the upper troposphere, which were heavily laden with methane, might not be dynamically unstable, resulting in sudden overturns and erasing the situation favorable to moist convection. A second problem with this picture is that, to achieve a fully 2% mixing ratio in the stratosphere, the subsiding air would be laden with methane condensate, which might be inconsistent with the limits on the methane cloud optical depth. The new lower values of the stratospheric methane abundance, of order 0.005–0.5% detailed earlier alleviate this problem somewhat; also, optical depth might be lower if the particles in the subsiding region grow to sufficient size (for a given amount of methane).

Requirement (*c*) raises the issue of what sorts of dynamical processes occur at the base of the methane cloud. Processes to lift parcels a significant distance before buoyancy is achieved might involve large-scale wave motions or moist convection associated with the deeper hydrogen sulfide cloud. Stoker (1986) argued that, on Jupiter, moist convection in the water cloud could contribute heat necessary to initiate moist convection in the overlying ammonia cloud. The likelihood of analogous processes occurring

on Uranus and Neptune depends in part on the vigor of the internal heat source. Podolak et al (1990) point out that the small internal heat flux on Uranus would tend to inhibit vertical transport of heat and stabilize the atmosphere. On Neptune, the much larger internal heat source could act to provide the upwelling necessary to trigger buoyant moist convection. However, this is speculative. Alternatively, LH showed that if a rising parcel of moisture-laden gas could be supersaturated significantly before condensing, it would become buoyant essentially at the condensation level. Values needed are 20% over saturation or greater (ST). Such supersaturation requires that the atmosphere be relatively clear of dust in order for condensation to be inhibited. This again is speculative but cannot be ruled out a priori.

ST suggested a novel approach to achieving buoyancy—namely, by postulating the rise of relatively dry air against a wetter background. As noted above, the calculations of LH suggested the need for a background atmosphere saturated in methane to offset the molecular weight penalty; ST generalized this by noting that any parcel drier than the background will rise. They tracked the parcel from the environmental methane cloud base to the point at which condensation occurs; parcels with an initial relative humidity less than 70% reach the cloud condensation level and continue to move upwards after condensation (ST). ST proposed that precipitation processes could lead to subsidence of dry air, which will eventually cease subsiding as precipitation stops and then begin to rise again.

In both the ST and LH models, large velocities, in excess of 100 m s^{-1}, are built up in the ascending plumes. Both models require plume diameters to exceed about 10 kilometers to prevent entrainment of background air from squelching the upward motion in the troposphere. The high velocities, however, die away around the tropopause ($P < 0.11$ bars on Uranus, 0.1–0.2 bars on Neptune). The suggestion by LH that eddy diffusion might waft particles further upwards works only for small particles; as particles are wafted upwards in the column, they grow in size. In microns, particles of size $r = (50\ K/H)^{1/2}$ can be buoyed upward by an eddy coefficient K when the scale height is H. Micron-sized particles require eddy coefficients of 10^5 cm^2/s to remain suspended in the stratosphere so that they can sublimate. In the lowermost stratosphere K may be 10^3, implying that only very small particles (0.1 microns) can continue to move upwards.

ST proposed instead that the plumes carry the particles directly to the region where they evaporate, which, they argued, might require the level of the troposphere to be depressed in plume regions relative to the global average. The radio occultation profiles for Neptune suggest a sharper (and on ingress, lower) tropopause than for Uranus, and a steeper stratospheric

temperature gradient. This steeper gradient means that methane cloud particles do not need to be transported as far to get to a region where they can evaporate on Neptune, as opposed to Uranus. This represents another self-reinforcing situation, since the steeper gradient is due to the larger stratospheric methane abundance on Neptune. However, the steeper gradient also acts to kill the cloud buoyancy faster, so it may be no easier for plumes to place cloud particles at a given warm level in the Neptune stratosphere than in Uranus'.

The sort of calculations described above need to be repeated using the latest available temperature profiles, and including effects such as para-ortho conversion. The revised estimates for stratospheric methane on Neptune place less of a demand on the moist convective models in terms of the amount of methane which must be delivered to the stratosphere. ST calculate that 2000 plumes per hour must penetrate the Neptunian tropopause to supply the stratosphere with 2% methane, balanced against various loss processes. It would be of interest to recompute this number when the stratospheric methane abundance is better constrained. Finally, the style of convection in the region of the methane cloud on Uranus appears to involve thin layers—a stable situation created or maintained in part by the molecular weight layering of methane cloud condensation (Gierasch & Conrath 1987). Is Neptune the same, or does its higher heat flow trigger moist convective processes which disrupt the layering and are self-sustaining? Is the absence of observable lightning, in contrast to Jupiter, a significant constraint on the vigor of methane moist convection (Borucki & Pham 1992)? Would such processes disrupt the apparently gentle meridional flow implied by the IRIS temperature maps and the observed zonal cloud motion? These questions, and others about the style of energy transport in the tropospheres of these planets, are well worth pursuing.

Origins of the Ice Giants

The currently favored model for the formation of the giant planets begins in a disk of hydrogen gas and dust that is now generally understood to be a frequent complement to newly forming stars (e.g. Beckwith & Sargent 1992). The process for each planet is initiated by the agglomeration ("accretion") of rock and ice grains which have condensed out or fallen inward from the surrounding molecular cloud to form a core, around which the hydrogen-helium gas begins to be gravitationally attracted. The density of the gas envelope continues to rise as more solid material is added to the core; eventually the gas envelope density becomes sufficiently high that much of the solid material simply sublimes and becomes part of the envelope. The details of the accretion of the bulk of the gaseous envelope

is unclear; whether a hydrodynamic collapse occurs at a critical core mass (Mizuno 1980), or the accretion rate of the envelope simply becomes much larger than that of the core (Bodenheimer & Pollack 1986), remains uncertain. In any event the formation process requires seeding by solid material, and now is not thought to be a result of direct instability in the nebular gas.

It is clear that, for Jupiter and Saturn, the accretion of the gaseous component occurred at a time when plenty of nebular gas was available; the much smaller hydrogen-helium complement in Uranus and Neptune argues that the core accretion was delayed to a time when little nebular gas was available (Podolak et al 1992). Interior models of Uranus and Neptune which are fitted to gravitational moment and rotational data are limited in their ability to determine uniquely the amounts of X, Y, and rock-forming versus ice-forming Z-elements.

The best-fitting models all have small cores of Z-elements, surrounded by primarily Z-element mantles of decreasing density and thin hydrogen-helium envelopes. Recent detailed models suggest that only 1/3 or less of the free hydrogen (not bound to Z-elements) and helium is in the envelope; the rest is mixed in the mantle of both planets (Hubbard et al 1991). This intermingling of the Z-elements and hydrogen-helium supports the above picture of accretion of gas and solid material simultaneously, with Z-element material evaporating in the gas at later times during formation. It is to be emphasized that, other than the higher bulk density of Neptune, the measured physical parameters of these bodies lead to similar internal structure models; i.e. sufficient uncertainty exists in the observed data and basic modeling parameters that one cannot argue for qualitatively different internal models for the two bodies.

The source of the measured internal energy for Uranus and Neptune is the original accumulation of material. The gravitational binding energy Ω of a spherical body assembled from material at infinite separation and initially at rest is $\Omega = -qGM^2/a$, where a is the body's radius, and q is a constant which depends on the interior mass distribution (Podolak et al 1992). Timescales of planet formation, based on modeling and astrophysical evidence (Levy & Lunine 1992), are sufficiently short that little of the energy Ω was radiated into space during formation; hence Ω represents the initial thermal content of the body. Now the thermal evolution of the planet to the present (4.5 billion years after formation) and the value of Ω yield a predicted effective temperature T_e (including insolation) at present. If the measured effective temperature T_e' is of order T_e, then the simple model of rapid formation and slow leakage of heat outward by efficient convective transport is supported. If $T_e' > T_e$, then additional sources of internal energy are present. This is the case on Jupiter and Saturn, where

helium appears to be phase separating from hydrogen in the deep interior, releasing additional gravitational energy (Stevenson & Salpeter 1977). The hydrogen and helium in Uranus and Neptune are not predicted to phase separate at the pressures relevant to their interiors. If $T_e' < T_e$, some process is impeding the effective removal of heat, or the planet formed very slowly and in such a way that a significant fraction of the virialized energy of collapse leaked out during formation (Podolak et al 1992).

For both Uranus and Neptune the predicted effective temperature is larger than the measured value. This suggested initially that perhaps these bodies formed very slowly. However, more recent models summarized in Podolak et al (1992) indicate that this is unlikely, and the answer may lie in stable stratification through the bulk of the interior, which tends to make the removal of heat an inefficient process (D. J. Stevenson, unpublished). The mismatch between predicted and measured effective temperature is larger for Uranus than for Neptune. Therefore, the suppression of convection by layering must be more severe in Uranus than Neptune. Uranus may also suffer an insulating effect from its closer proximity to the Sun, its high obliquity, and the long tropospheric radiative time constant. Together these may act to suppress the internal heat flux at all latitudes on Uranus, whereas on Neptune, some internal heat is shunted towards high latitudes (Podolak et al 1990; see also Hubbard 1978). The insolation effect is, however, likely to be secondary in explaining the different heat fluxes of the two bodies.

What is the connection between the atmospheres and interior/origins issues for Uranus and Neptune? Firstly, measurement of the atmospheric D/H ratio and helium abundances provide some constraints on the amount of internal mixing and reequilibration of material in the interiors, while abundances of disequilibrium species such as CO yield information on the vigor of convection at about the kilobar level in the atmosphere. Second, the models presented above for the formation of Uranus and Neptune imply that most of the Z-element material in these two planets was derived from solid rock and ice particles in the solar nebula, which according to some current dynamical models may still be around in relict form today in long-period comets (Duncan & Quinn 1992). Hence there should be links between the elemental and isotopic abundances in Uranus and Neptune and those in some comets.

The helium abundances in the giant planets ought to reflect the original hydrogen to helium ratio in the solar nebular gas, which is expected to be typical of the value in the Galaxy 4.5 billion years ago. While a wealth of literature exists on what exactly the primordial value ought to be, $0.27 < Y < 0.28$ seem to be favored currently (Fegley et al 1991). The number for Uranus is well within this range; the Neptune number may

indicate a slight enhancement. Alternatively for Neptune, if most of the nitrogen is in the form of N_2, the helium abundance is consistent with the primordial value (Marten et al 1993). The separation of helium from hydrogen in the deep interiors of Jupiter and Saturn depletes atmospheric helium, and the values for those objects reflect such depletion. Any enhancement in helium in the Neptune atmosphere is likely to result from the incorporation of carbon and nitrogen in the forming planet in oxidized form, i.e. primarily as CO and N_2 rather than as CH_4 and NH_3. Thermochemical equilibrium in the deep interiors then reduces the CO and N_2 at the expense of molecular hydrogen. The amount of molecular hydrogen taken up depends upon the amount of icy material accommodated in the interior and the composition of the carbon and nitrogen bearing species. While interior models constrain the total Z-element abundance in the interior fairly well, the ratio of the rock-forming elements to the ice-forming elements is poorly determined and is usually estimated from solar abundances or nebular models. With a guess as to the rock-ice ratio, one can use cometary material as a guide to the molecular composition; most of the carbon in comets is in the form of CO, CO_2, and nonvolatile reduced carbon. The relative amounts of ammonia, molecular nitrogen, and nitrogen in involatile phases is more poorly determined (Mumma et al 1992).

Finally, whether the consumption of hydrogen in the deep interior is reflected in the tropospheric helium abundance depends upon how much mixing occurs within the bulk interior and between the interior and outer hydrogen-helium envelope. Because of these uncertainties, one cannot predict a specific value for the helium enhancement in Neptune. A maximum enhancement in the helium abundance of roughly 10% is possible (Fegley et al 1991), assuming full interior mixing and all carbon and nitrogen coming into the planets in oxidized form. A smaller number (3–9%) was derived by Pollack et al (1986) under the assumption that the incoming planetesimals were carbonaceous chondrites, with no contribution from carbon and nitrogen trapped in ices. Given the error bars on the Neptune helium abundance, either model is possible and intermediate models (such as a combination of ice and rock with some carbon in reduced form) also satisfy the data. One additional source of hydrogen consumption is dissolution in the water cloud, but this yields an effect of only 2% enhancement in the helium-to-hydrogen ratio (Fegley & Prinn 1986).

If it were possible to show that the helium abundance in Neptune is enhanced relative to the Uranus value, which is solar, it leads to the intriguing question as to why helium enhancement occurred only on Neptune. One answer is tied to the heat flow issue: If Uranus is stably layered (e.g. by compositional gradients) such that much of the internal heat is

prevented from escaping, mixing in the interior would also be severely limited. The hydrogen-helium composition of the outer envelope would then be decoupled from chemical processes in the interior, and not reflect any helium enhancement. If Neptune were more fully mixed, consistent with its higher heat flow, the effects of hydrogen incorporation would be reflected in the outermost atmosphere. Until the error bars on the helium abundance can be reduced, unfortunately, one cannot use the current values with their error bars to argue strongly for this idea.

The error bars on the D/H ratio in the Uranian and Neptunian atmospheres, given earlier, are rather large but nonetheless indicate an enhancement over the value predicted for Population I hydrogen gas 4.5 billion years ago. Recalling that Z-element molecules are heavily enriched in deuterium in molecular clouds, largely due to ion-molecule reactions (Van Dishoeck et al 1992), introduction of these ices into the forming Uranus and Neptune, followed by exchange with hydrogen, results in an enhanced D/H ratio in the bulk gas. One can use the D/H values to estimate the amount of icy material brought into Uranus and Neptune, assuming full mixing in the interiors and a D/H ratio in primitive ices (using comet Halley data) of 10 times the solar value. Podolak et al (1992) determined that the lower limits on the D/H ratio in Uranus and Neptune, discussed earlier, do not require much icy material in the two planets, only an amount about equal to the hydrogen-helium mass (recall that the total Z-element mass in the planets is fairly well fixed by the interior modeling and gravitational moments, so that less ice is compensated by more rock). The upper values for D/H correspond to the Halley enhancement, and therefore requires that very little free (i.e. protoplanetary disk gas) hydrogen and helium were incorporated in Uranus and Neptune; most of the hydrogen in these planets would then have been derived from that in the icy material: from Z-element molecules (such as CH_4) and from some hydrogen possibly trapped in the ice structure (Lunine & Stevenson 1985).

The hypothesis of severe layering in Uranus argues for a different D/H ratio in that atmosphere than in a well-mixed Neptune, with the former having a value closer to the cosmic abundance. However, determining this is a highly model-dependent exercise, and the large error bars on the observed D/H ratios in Uranus, Neptune, Halley, and other outer solar system objects make this effort unconstrained at present.

One final intriguing constraint is the sulfur abundance. The apparent requirement from the ground-based microwave data to have an enhanced S/N ratio in the atmosphere in order to sequester ammonia puts some constraints on planetesimal composition. Carbonaceous chondrites have S/N = 10, in contrast with S/N = 0.2 in solar abundance (Fegley et al 1991). If the interpretation of the microwave observations is correct

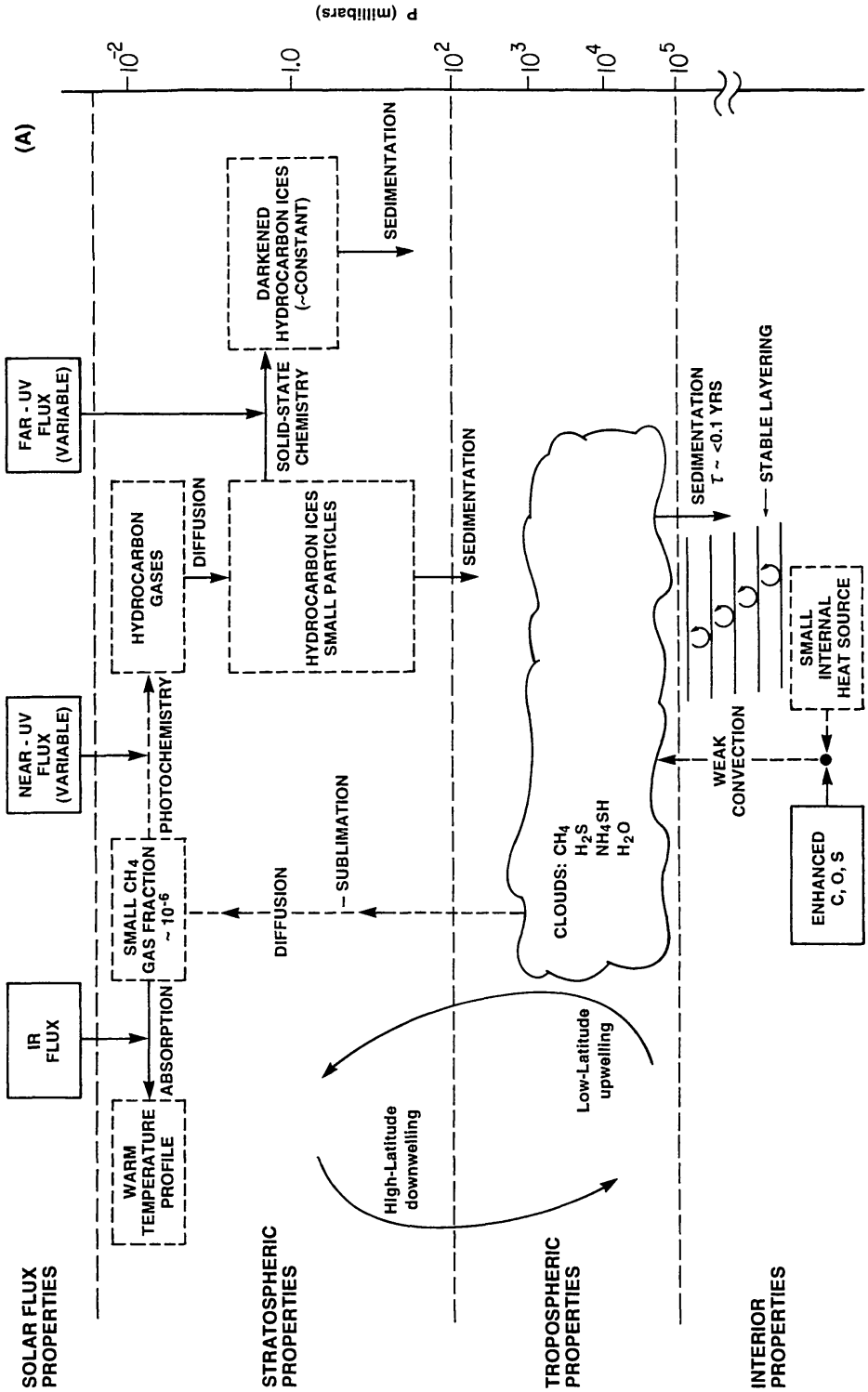

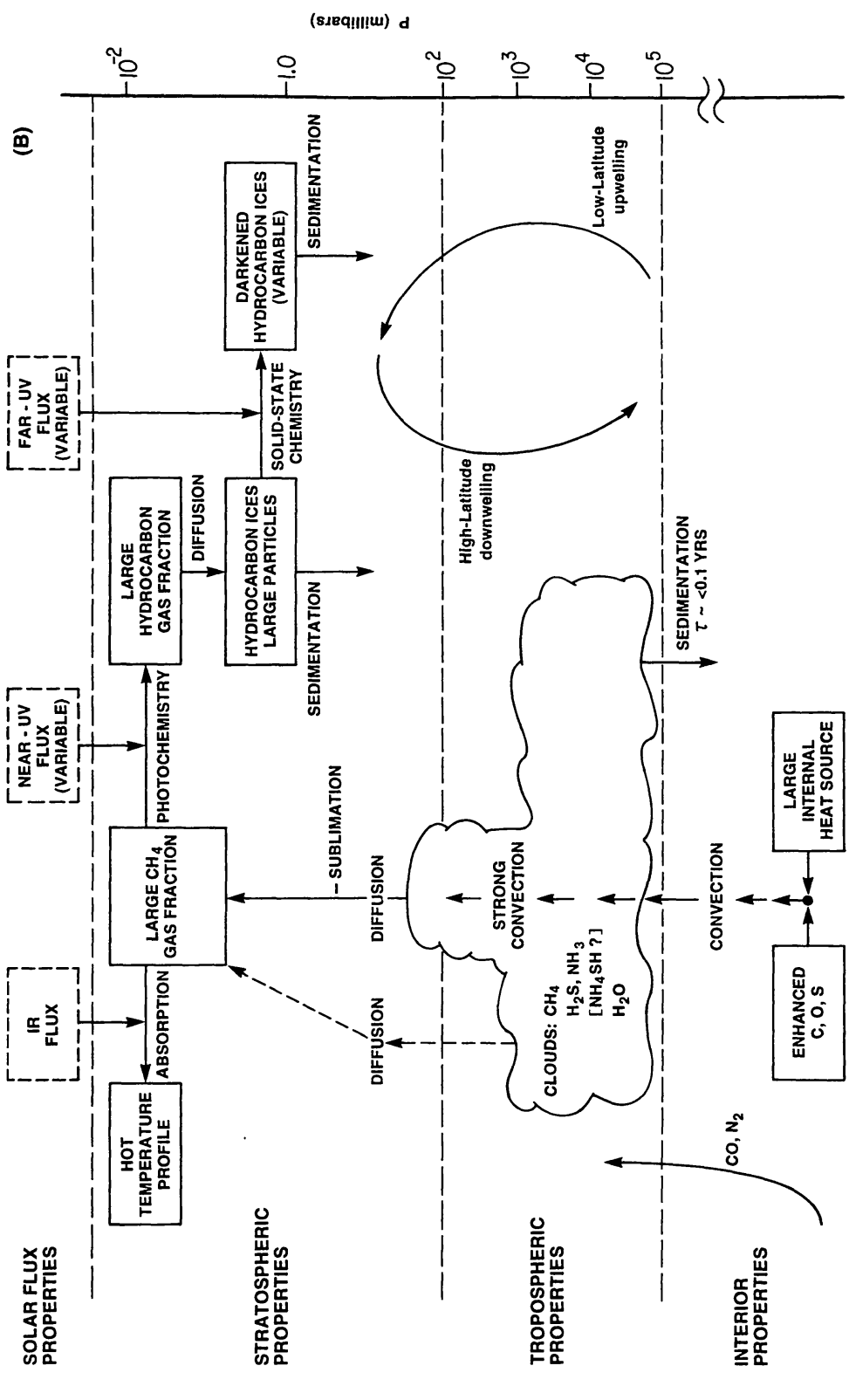

Figure 9 Selected chemical and physical processes in the atmospheres of (*A*) Uranus and (*B*) Neptune, modified from Baines & Smith (1990). The various levels in the atmosphere are arranged according to pressure, on a logarithmic scale. Boxes that are dashed indicate processes which are weaker compared to the corresponding ones on the other planet.

(S/N = 5; de Pater et al 1991), it imposes constraints on the amount of nitrogen-bearing ices that can be accreted into Uranus and Neptune early on, since the ice will tend to enhance the nitrogen abundance above the value in chondrites. Further work to put the microwave observations on firmer footing is therefore of great interest; a lingering uncertainty will be the S/N value in ices, but work on comet composition may further constrain that figure (Mumma et al 1992).

The uncertainties cited above, as well as in the determination of the nitrogen and oxygen enhancements in the atmosphere, prevent the exercises described above from being well-constrained at present. Further improvements in the precision of determining the tropospheric composition may eventually lead to important insights on the nature of the original planetesimals from which these ice giants formed, and on current differences in their structure and modes of energy transport.

CONCLUSION

This article closes not with a long recitation of conclusions, but rather with Figure 9, which illustrates some of the processes and characteristics of the Uranian and Neptunian atmospheres. Most intriguing about these two bodies are their various similarities and differences: internal heat flow, internal structure, surface appearance, and atmospheric composition. It is not yet understood why the measured internal heat flows are so different for the two bodies, how deep this difference extends, and what this means for the relationship of atmospheric composition to bulk interior properties. Because these planets are mostly made of rock- and ice-forming elements, the compositions of the atmospheres contain clues to the nature of the material out of which solid bodies in the outer solar system formed. Until some understanding of the connection between the atmospheres and interiors of these objects is achieved, these clues are of limited use. The best of all possible worlds might be if Uranus were heavily layered, so that its atmosphere is isolated from interior processes, while Neptune's atmosphere is well connected to the interior by convection. This complementary pair would then tell us much about the original planet-forming matter and subsequent history, perhaps even answer the question of why, as a set, Uranus and Neptune are so different from the gas giants Jupiter and Saturn. As with the rest of the universe, however, the true comparative nature of Uranus and Neptune is likely more complicated.

The future of further observational progress looks bright. New infrared and optical detectors, large telescopes, and space-borne platforms should improve our understanding of the atmospheric compositions and enable better tracking of cloud features from Earth. Observations with new gen-

eration facilities over decades will reveal the seasonal patterns in these two atmospheres which are now so poorly understood. Laboratory experiments at high pressures and further chemical kinetics studies should reduce the uncertainties inherent in both interior and atmospheric models. NASA has studied a mission to orbit Neptune and release a probe into the planet's atmosphere, which would finalize the answers to several compositional questions. Unfortunately, with current propulsive technologies, flight times are well in excess of a decade, which are politically if not technically prohibitive. Such a mission may well have to await the implementation of nuclear electric propulsion. In the meantime, there is much to do in learning more about the Solar System's distant blue ice giants.

ACKNOWLEDGMENTS

The vigor of this field is reflected in the number and quality of comments received on an earlier version of the manuscript. Corrections and suggestions by S. Atreya, K. Baines, J. Bergstralh, B. Bézard, F. M. Flasar, J. Friedson, D. Gautier, H. Hammel, W. B. Hubbard, D. M. Hunten, G. Orton, T. Owen, M. Podolak, C. Sagan, R. Samuelson, D. F. Strobel, R. V. Yelle, and Y. L. Yung were greatly appreciated. The preparation of this article was supported by NASA Grant NAGW-1039. This paper is contribution number 92-46 of the Theoretical Astrophysics Program, University of Arizona.

Literature Cited

Allison, M., Beebe, R., Conrath, B. J., Hinson, D. P., Ingersoll, A. P. 1991. See Bergstralh et al 1991, pp. 253–95
Anders, E., Grevesse, N. 1989. *Geochim. Cosmochim. Acta* 53: 197–214
Appleby, J. F. 1986. *Icarus* 65: 383–405
Atreya, S. K. 1984. See Bergstralh 1984, pp. 55–88
Atreya, S. K., Ponthieu, J. J. 1983. *Planet. Space Sci.* 33: 939–44
Atreya, S. K., Sandel, B. R., Romani, P. N. 1991. See Bergstralh et al 1991, pp. 110–46
Baines, K. H., Bergstralh, J. T. 1986. *Icarus* 65: 406–41
Baines, K. H., Hammel H. B. 1992. *Bull. Am. Astron. Soc.* 24: 973
Baines, K. H., Smith, W. H. 1990. *Icarus* 85: 65–108
Beatty, J. K., O'Leary, B., Chaikin, A., eds. 1981. *The New Solar System.* Cambridge, Mass.: Sky. 224 pp.
Beckwith, S. V. W., Sargent, A. 1992. See Levy & Lunine 1992, 521–41
Bergstralh, J. T., ed. 1984. *Uranus and Neptune.* Washington DC: NASA Conf. Publ. 2330. 627 pp.
Bergstralh, J. T., Miner, E. D., Matthews, M., eds. 1991. *Uranus.* Tucson: Univ. Ariz. Press. 1076 pp.
Bézard, B., Romani, P. N., Conrath, B. J., Maguire, W. C. 1991. *J. Geophys. Res.* 96: 18,961–75
Bishop, J., Atreya, S. K., Romani, P. N., Sandel, B. R., Herbert, F. 1992. *J. Geophys. Res.* 97: 11,681–94
Bodenheimer, P., Pollack, J. B. 1986. *Icarus* 67: 391–408
Borucki, W. J., Pham, P. C. 1992. *Icarus* 99: 384–89
Borysow, J., Trafton, L., Frommhold, L., Birnbaum, G. 1985. *Ap. J.* 296: 644–54
Borysow, A., Frommhold, L. 1986. *Ap. J.* 304: 849–65
Borysow, J., Frommhold, L., Birnbaum, G. 1988. *Ap. J.* 326: 509–15
Broadfoot, A. L., Herbert, F., Holberg, J. B., Hunten, D. M., Kumar, S., et al. 1986. *Science* 233: 74–79
Broadfoot, A. L., Atreya, S. K., Bertaux, J.

L., Blamont, J. E., Dessler, A. J., et al. 1989. *Science* 246: 1459–66
Carlson, B. E., Prather, M. J., Rossow, W. B. 1987. *Ap. J.* 321: L97–L101
Chamberlain, J. W., Hunten, D. M. 1987. *Theory of Planetary Atmospheres: An Introduction to their Physics and Chemistry*. Orlando, Fla.: Academic. 481 pp.
Clayton, D. D. 1968. *Principles of Stellar Evolution and Nucleosynthesis*. New York: McGraw-Hill. 612 pp.
Conrath, B., Gautier, D., Hanel, R., Lindal, G., Marten, A. 1987. *J. Geophys. Res.* 92: 15,003–10
Conrath, B. J., Hanel, R. A., Samuelson, R. E. 1989. In *Origin and Evolution of Planetary and Satellite Atmospheres*, ed. S. K. Atreya, J. B. Pollack, M. S. Matthews, pp. 513–38. Tucson: Univ. Ariz. Press
Conrath, B. J., Flasar, F. M., Gierasch, P. 1991a. *J. Geophys. Res.* 96: 18,931–39
Conrath, B. J., Gautier, D., Lindal, G. F., Samuelson, R. E., Shaffer, W. A. 1991b. *J. Geophys. Res.* 96: 18,907–19
Conrath, B. J., Pearl, J. C., Appleby, F., Lindal, G. F., Orton, G. S., Bézard, B. 1991c. See Bergstralh et al 1991, pp. 204–52
Conrath, B. J., Gautier, D., Owen, T. C., Samuelson, R. C. 1993. *Icarus* in press
de Bergh, C., Lutz, B. L., Owen, T., Brault, J., Chauville, J. 1986. *Ap. J.* 311: 501–10
de Bergh, C., Lutz, B. L., Owen, T., Maillard, J.-P. 1990. *Ap. J.* 355: 661–66
de Pater, I., Romani, P. N., Atreya, S. K. 1991. *Icarus* 91: 220–33
Duncan, M. J., Quinn, T. 1992. See Levy & Lunine 1992, pp. 1371–94
Fegley, B. Jr., Gautier, D., Owen, T., Prinn, R. G. 1991. See Bergstralh et al 1991, pp. 147–203
Fegley, B. Jr., Prinn, R. 1986. *Ap. J.* 307: 852–65
Flasar, F. M., Conrath, B. J., Gierasch, P. J., Pirraglia, J. A. 1987. *J. Geophys. Res.* 92: 15,011–18
Friedson, J., Ingersoll, A. P. 1987. *Icarus* 69: 135–56
Gautier, D., Owen, T. 1989. In *Origin and Evolution of Planetary and Satellite Atmospheres*, ed. S. K. Atreya, J. B. Pollack, M. S. Matthews, pp. 487–512. Tucson: Univ. Ariz. Press
Gierasch, P. J., Conrath, B. J. 1987. *J. Geophys. Res.* 92: 15,019–29
Grevesse, N., Lambert, D. L., Sauval, A. J., Van Dishoeck, E. F., Farmer, C. B., Norton, R. H. 1991. *Astron. Astrophys.* 242: 488–95
Hammel, H. B. 1989. *Icarus* 80: 14–22
Hammel, H. B., Baines, K. H., Bergstralh, J. T. 1989. *Icarus* 80: 416–38
Hammel, H. B., Lawson, S. L., Harrington, J., Lockwood, G. W., Thompson, D. T., Swift, C. 1992a. *Icarus* 99: 363–67
Hammel, H. B., Young, L. A., Hackwell, J., Lynch, D. K., Russell, R., Orton, G. S. 1992b. *Icarus* 99: 347–52
Hanel, R., Conrath, B., Flasar, F. M., Kunde, V., Maguire, W., et al. 1986. *Science* 233: 70–74
Herbert, F., Sandel, B. R., Yelle, R. V., Holberg, J. B., Broadfoot, A. L., et al. 1987. *J. Geophys. Res.* 92: 15,093–109
Hertzberg, G. 1952. *Ap. J.* 115: 337–40
Hess, S. L. 1979. *Introduction to Theoretical Meteorology*. Huntington, NY: Kriegal
Hofstadter, M., Muhleman, D. O. 1988. *Icarus* 81: 396–412
Hubbard, W. B. 1978. *Icarus* 35: 177–81
Hubbard, W. B., McFarlane, J. J. 1980. *Icarus* 44: 676–82
Hubbard, W. B., Nicholson, P. D., Lellouch, E., Sicardy, B., Brahicm, A., et al. 1987. *Icarus* 72: 635–46
Hubbard, W. B., Nellis, W. J., Mitchell, A. C., Holmes, N. C., Limaye, S. S., McCandless, P. C. 1991. *Science* 253: 648–51
Hunten, D. M. 1974. In *The Atmosphere of Uranus*, ed. D. M. Hunten. pp. 1–7. Washington, DC: NASA
Joyce, R. R., Pilcher, C. B., Cruikshank, D. P., Morrison, D. 1977. *Ap. J.* 214: 657–62
Khare, B. N., Sagan, C., Thompson, W. R., Arakawa, E. T., Votaw, P. 1987. *J. Geophys. Res.* 92: 15,067–82
Kostiuk, T., Romani, P., Espenak, F., Bézard, B. 1992. *Icarus* 99: 353–62
Lane, A. L., West, R. A., Hord, C. W., Nelson, R. M., Simmons, K. E., et al. 1989. *Science* 246: 1450–54
Levy, E. H., Lunine, J. I., eds. 1992. *Protostars and Planets III*. Tucson: Univ. Ariz. Press. 1596 pp.
Limaye, S. S., Sromovsky, L. A. 1991. *J. Geophys. Res.* 96: 18,941–60
Lindal, G. F. 1992. *Astron. J.* 103: 967–82
Lindal, G. F., Lyons, J. R., Sweetnam, D. N., Eshleman, V. R., Hinson, D. P., Tyler, G. L. 1987. *J. Geophys. Res.* 92: 14,987–5001
Lindal, G. F., Lyons, J. R., Sweetnam, D. N., Eshleman, V. R., Hinson, D. P., Tyler, G. L. 1990. *Geophys. Res. Lett.* 17: 1733–36
Lockwood, G. W., Lutz, B. L., Thompson, D. T., Warnock, A. III. 1983. *Ap. J.* 266: 402–14
Lockwood, G. W., Thompson, D. T., Hammel, H. B., Birch, P., Candy, M. 1991. *Icarus* 90: 299–307
Lunine J. I., Hunten, D. M. 1989. *Planet. Space Sci.* 37: 151–66 (LH)

Lunine, J. I., Stevenson, D. J. 1985. *Ap. J. Suppl.* 58: 493–531
Lutz, B. L., Owen, T., Cess. R. D. 1976. *Ap. J.* 203: 541–51
Lutz, B. L., Owen, T. C., de Bergh, C. 1990. *Icarus* 86: 329–35
Maguire, W. 1992. *Bull. Am. Astron. Soc.* 24: 974
Marten, A., Gautier, D., Owen, T., Sanders, D. B., Matthews, H. E., et al. 1993. *Ap. J.* 406: 285–97
Miner, E. D. 1991. *Uranus: The Planet, Rings and Satellites*. New York: Ellis Horwood. 334 pp.
Mizuno, H. 1980. *Prog. Theor. Phys.* 64: 544–57
Moses, J. I. 1992. *Icarus* 99: 368–83
Moses, J. I., Allen, M., Yung, Y. L. 1992. *Icarus* 99: 318–46
Mumma, M. J., Weismann, P., Stern, A. S. 1992. See Levy & Lunine 1992, pp. 1177–252
Orton, G. S., Appleby, J. F. 1984. In *Uranus and Neptune*, ed. J. Berstralh, pp. 89–155. Washington, DC: NASA Conf. Publ. 2330
Orton, G. S., Griffin, M. J., Ade, P. A. R., Nolt, I. G., Radostitz, J. V., et al. 1986. *Icarus* 67: 289–304
Orton, G. S., Aitken, D. K., Smith, C., Roche, P. F., Caldwell, J., Snyder, R. 1987. *Icarus* 70: 1–12
Orton, G. S., Baines, K. H., Caldwell, J., Romani, P., Tokunaga, A. T., West, R. A. 1990. *Icarus* 85: 257–65
Orton, G. S., Lacy, J. H., Achtermann, J. M., Parmar, P., Blass, W. E. 1992. *Icarus* 100: 541–55
Owen, T. C., Lutz, B. L., de Bergh, C. 1986. *Nature* 320: 244–46
Parkinson, C. D., McConnell, J., Sandel, B. R., Yelle, R. V., Broadfoot, A. L. 1990. *Geophys. Res. Lett.* 17: 1709–12
Pearl, J. C., Conrath, B. J. 1991. *J. Geophys. Res.* 96: 18,921–30
Podolak, M., Reynolds, R. T., Young, R. 1990. *Geophys. Res. Lett.* 17: 1737–40
Podolak, M., Hubbard, W. B., Pollack, J. B. 1992. See Levy & Lunine 1992, pp. 1109–47
Pollack, J. B., Podolak, M., Bodenheimer, P., Christofferson, B. 1986. *Icarus* 67: 409–43
Pollack, J. B., Rages, K., Pope, S. K., Tomasko, M. G., Romani, P. N., Atreya, S. K. 1987. *J. Geophys. Res.* 92: 15,037–65
Pryor, W. R., West, R. A., Simmons, K. E., Delitsky, M. 1992. *Icarus* 99: 302–17
Rages, K. A., Pollack, J. B. 1988. *Bull. Am. Astron. Soc.* 20: 821
Romani, P. N., Atreya, S. K. 1989. *Geophys. Res. Lett.* 16: 941–44
Romani, P. N., Lellouch, E., Rosenqvist, J., Encrenaz, Th., Paubert, G. 1992. *Bull. Am. Astron. Soc.* 24: 972
Rosenqvist, J., Lellouch, E., Romani, P. N., Paubert, G., Encrenaz, T. 1992. *Ap. J. Lett.* 392: L99–L102
Smith, B. A., Soderblom, L. A., Beebe, R. F., Bliss, D., Boyce, J. M., et al. 1986. *Science* 233: 43–64
Smith, B. A., Soderblom, L. A., Banfield, D., Barnet, C., Basilevsky, A. T., et al 1989. *Science* 246: 1422–49
Smith, W. H., Conner, C. P., Baines, K. H. 1990. *Icarus* 85: 58–64
Sromovsky, L. A., Limaye, S. S. 1992. *Bull. Am. Astron. Soc.* 24: 973
Stevens, M. H., Strobel, D. E., Herbert, F. 1993. *Icarus* 101: 45–63
Stevenson, D. J., Salpeter, E. E. 1977. *Ap. J. Suppl.* 35: 239–61
Stoker, C. R. 1986. *Icarus* 67: 106–25
Stoker, C. R., Toon, O. B. 1989. *Geophys. Res. Lett.* 16: 929–32 (ST)
Strobel, D. F., Yelle, R. V., Shemansky, D. E., Atreya, S. K. 1991. See Bergstralh et al 1991, pp. 65–109
Summers, M. E., Strobel, D. F. 1989. *Ap. J.* 346: 495–508
Trafton, L. M., Ramsay, D. A. 1980. *Icarus* 41: 423–29
Tyler, G. L., Sweetnam, D. N., Anderson, J. D., Campbell, J. K., Eshleman, V. R., et al. 1986. *Science* 233: 79–84
Tyler, G. L., Sweetnam, D. N., Anderson, J. D., Borutzki, S. E., Campbell, J. K., et al. 1989. *Science* 246: 1466–73
Van Dishoeck, E. F., Blake, G. A., Draine, B. T., Lunine, J. I. 1992. See Levy & Lunine 1992, pp. 163–241
Warwick, J. W., Evans,D. R., Romig, J. H., Sawyer, C. B., Desch, M. D., et al. 1986. *Science* 233: 102–6
Warwick, J. W., Evans, D. R., Peltzer, G. R., Peltzer, R. G. Romig, J. H., et al. 1989. *Science* 246: 1498–501
West, R. A., Lane, A. L., Hord, C. W., Esposito, L. W., Simmons, K., et al. 1987. *J. Geophys. Res.* 92: 15,030–36
West, R. A., Baines, K. H., Pollack, J. B. 1991. See Bergstralh et al 1991, pp. 296–324
Yelle, R. V., Herbert, F., Sandel, B. R., Vervack, R. J. Jr., Wentzel, T. M. 1993. *Icarus* In press
Zharkov, V. N., Gudkova, T. V. 1991. *Ann. Geophys.* 9: 357–66